REPORT DOCUMENTATION PAGE

Form Approved
OMB No. 0704-0188

1. REPORT DATE *(DD-MM-YYYY)*	2. REPORT TYPE	3. DATES COVERED *(From - To)*
05/10/2019	Master's Thesis	09/24/2018 - 05/10/2019

4. TITLE AND SUBTITLE
Quantification of Extreme Event Statistics in Ship Design

5a. CONTRACT NUMBER
N/A

5b. GRANT NUMBER
N/A

5c. PROGRAM ELEMENT NUMBER
N/A

6. AUTHOR(S)
Udit Rathore

5d. PROJECT NUMBER
N/A

5e. TASK NUMBER
N/A

5f. WORK UNIT NUMBER
N/A

7. PERFORMING ORGANIZATION NAME(S) AND ADDRESS(ES)
Massachusetts Institute of Technology
77 Massachusetts Ave.,
Cambridge, MA 02139

8. PERFORMING ORGANIZATION REPORT NUMBER
N/A

9. SPONSORING/MONITORING AGENCY NAME(S) AND ADDRESS(ES)
N/A

10. SPONSOR/MONITOR'S ACRONYM(S)
N/A

11. SPONSOR/MONITOR'S REPORT NUMBER(S)
N/A

12. DISTRIBUTION/AVAILABILITY STATEMENT
DISTRIBUTION A. Approved for public release: distribution unlimited

13. SUPPLEMENTARY NOTES

14. ABSTRACT

This thesis builds on previous work at the MIT Stochastic Analysis and Non-linear Dynamics (SAND) lab for the quantification of extreme events using wave groups. By separating the event probability from the physics models, we are able to capture rare events in ship motion and loading conditions for a modest computational cost. Improvements to the wave groups methodology ensured the slope and amplitude of the incident waves reflected the waves encountered in a given wave spectrum. The remaining discussion explores the value of a near-real-time risk analysis tools in reference to ship design and ship operations, with unique application to Navy and Commercial Vessels.

15. SUBJECT TERMS
Risk-based Ship Design, Wave Groups, Operational Efficiency, Extreme Event, Monte Carlo, Risk-related Design,

16. SECURITY CLASSIFICATION OF:			17. LIMITATION OF ABSTRACT	18. NUMBER OF PAGES	19a. NAME OF RESPONSIBLE PERSON
a. REPORT	b. ABSTRACT	c. THIS PAGE			MIT Academic Officer
					19b. TELEPHONE NUMBER *(Include area code)*
U	U	U	UU	86	617-253-4339

Quantification of Extreme Event Statistics in Ship Design

by

Uditbhan S. Rathore

B.S., U.S. Naval Academy, 2012

Submitted to the Department of Mechanical Engineering and
System Design and Management Program in partial fulfillment of the requirements for the degrees of

Master of Science in Engineering and Management

and

Naval Engineer

at the

MASSACHUSETTS INSTITUTE OF TECHNOLOGY

June 2019

Author .....
Department of Mechanical Engineering and
System Design and Management Program
May 10, 2019

Certified by .....
Themistoklis P. Sapsis
Associate Professor of Mechanical and Ocean Engineering
Thesis Supervisor

Certified by .....
Bryan R. Moser
Academic Director and Sr. Lecturer, System Design and Management
Thesis Supervisor

Accepted by .....
Joan Rubin
Executive Director, System Design and Management

Accepted by .....
Nicolas Hadjiconstantinou
Chairman, Committee on Graduate Students

Quantification of Extreme Event Statistics in Ship Design

by

Uditbhan S. Rathore

Submitted to the Department of Mechanical Engineering and
System Design and Management Program
on May 10, 2019, in partial fulfillment of the
requirements for the degrees of
Master of Science in Engineering and Management
and
Naval Engineer

Abstract

Increased operational demands on Navy vessels extend time at sea and service life, making the accurate prediction of catastrophic failures increasingly challenging. The high value of these capital assets puts great pressure on designers and decision-makers as they work towards preventing such failures while balancing both engineering and material cost. The current method for the quantification of extreme events is direct Monte Carlo simulation supplemented by complex statistical models. When such models are not sufficiently bound by physics-based simulation, the noise of statistical uncertainty quickly overpowers the response predictions for rare events.

This thesis builds on previous work at the MIT Stochastic Analysis and Non-linear Dynamics (SAND) lab for the quantification of extreme events using wave groups. By separating the event probability from the physics models, we are able to capture rare events in ship motion and loading conditions for a modest computational cost. Improvements to the wave groups methodology ensured the slope and amplitude of the incident waves reflected the waves encountered in a given wave spectrum. The remaining discussion explores the value of a near-real-time risk analysis tools in reference to ship design and ship operations, with unique application to Navy and commercial vessels.

Thesis Supervisor: Themistoklis P. Sapsis
Title: Associate Professor of Mechanical and Ocean Engineering

Thesis Supervisor: Bryan R. Moser
Title: Academic Director and Sr. Lecturer, System Design and Management

Acknowledgments

I would like to thank my advisers, Professor Themistoklis Sapsis and Bryan Moser for their patience and encouragement through this process. This document would not have been possible without their positive attitude and guidance. Professor Sapsis took time during his sabbatical to help formulate this project and provided invaluable technical guidance along the way. Bryan was a valuable sounding board, whose perspective gave structure to put my analysis in larger context during my thesis-writing process.

From Naval Surface Warfare Center-Carderock Division, Ken Weems and Vadim Belenky, without whose time, interest, background, experience, and knowledge, this document would not have been possible.

This thesis is the continuation of work completed by members of the MIT Stochastic Analysis and Nonlinear Dynamics (SAND) lab. Kevin Stevens and Mustafa Mohamad provided the ground work this thesis was built upon. Their continued support though this process has helped me overcome many technical challenges.

I would also like to acknowledge the instructors and my cohorts in Naval Construction and Engineering (2N) and System Design and Management (SDM) programs. I have learned a tremendous amount working along side you. Your feedback has been invaluable over these past three years. Thank you for making this time enjoyable and memorable.

My entire experience here at MIT would not have been possible without the support of my wife, Needhee Rathore. From leaving San Diego to brave the Boston winters, to wedding planning and building a new life together, her support has been unwavering through the highs and lows of this journey. And as always, my parents, Monica and Abhai Rathore for their unconditional support and encouragement. I am here because of you all.

Contents

List of Figures

List of Tables

Chapter 1

Introduction

A statistical understanding of ocean waves has been fundamental to the design and monitoring of marine and naval structures due to the random nature of the seas. More specifically, the ability to understand the risk and frequency of catastrophic events have been topics of interest in numerous fields. In a practical sense, ship designers write specifications to deliver a product that will perform in the worst reasonable situation. The main problem they face is that these situations are very rare events; otherwise failures would shut down the industry. The proportion of catastrophic failures to the number of vessels at sea has shrunk in the past half century because of rule-based design standards and improved quality assurance practices. A catastrophic failure is in the realm of societally acceptable risk and risk probability, but the fiscal and operational cost of losing a capital asset like a Navy warship is still great. For example, it is accepted that a combatant naval vessel might be shot at during a conflict and the expectation is that within a scope of damage, the vessel should survive. Similarly, society expects that a cargo ship will deliver its cargo safely during a routine transit, but not necessarily while transiting through a hurricane. Therefore, heavy weather guidance systems exist; however, establishing what is acceptable risk is not a technical matter, nor in question. Risk that was acceptable 70 years ago is not necessarily acceptable today. The more appropriate question, and the question of this thesis, is whether a more efficient and accurate approach to the quantification of extreme events in ship design exists. If so, how would it affect ship design, ship

operations, and ongoing science?

The International Maritime Organization (IMO) took first steps in 2009 to shift the maritime industry from prescriptive design standards to a risk-based system. This shift was driven by the conflict between technological advances in manufacturing and computation with a design envelope that was limited by regulation. This foray into Risk-Based Ship Design (RBSD) is discussed further in Chapter 2 and provides the background for this work on the quantification of extreme events statistics on ship design. Traditionally, quantifying the risk using physics-based models has been a resource-intensive process. Designers and decision-makers get around this challenge by augmenting shorter physics simulations with statistical models, accepting a significant amount of uncertainty in the prediction of rare, catastrophic events. This study works to develop a method of characterizing the statistics of the rare events at a fraction of the computational cost.

1.1 Contributions

This study improves upon Wave Groups methodology developed at the MIT Stochastic Analysis and Non- Linear Dynamics (SAND) lab in an effort towards the quantification of extreme event statistics of ship motion and loading conditions. A blended approach of physics and statistical models was necessary to capture the probability and severity of rare events.

1.1.1 Risk-Based Ship Design

Scientific and technological advances and an overall improved technical capability have fueled innovation in the shipping sector to meet the demand for larger, more specialized, and more capable ships. For decades computational tools have allowed designers to replicate model testing, ship systems performance, and model ship process in a digital space. By integrating these decision support tools into the design process, it is now feasible for designers and decision makers to evaluate a much wider design space than ever before. The wave groups approach presented in this work

provides a deeper understanding of the probability of extreme events in ship motion and loading conditions to inform functional requirements of for a risk-based design approach.

1.1.2 Quantification of Risk in Ship Motion and Loading

The work presented in this thesis builds directly off previous work completed by members of the MIT SAND labs. Sapsis, Stevens and Mohamad provided the ground work for the application of the Wave Groups methodology and Probability-Decomposition-Synthesis (PDS) that enabled the worked presented here. The emphasis of this study was to capture the additional properties of the wave systems that produce the extreme events and reproduce them within the wave group simulations.

1.1.3 Industry Application

The final phase of the study is a discussion on the application of this approach for quantifying event statistics using on systems engineering principles. We considered the technical feasibility and barriers of entry for achieving a near-real-time risk decision support system based on wave groups. In the past decades, many attempts have been made to measure incident wave characteristics at sea; however, all attempts have been overwhelmed by the non-linearities of the sea and the ship's structure. Finally, we considered the applications of the Wave Groups methodology for the future of ship routing via decision support systems (DSS) driven by operational efficiency rather than operating limits, as they are today.

1.2 Organization

This thesis is divided in to three sections, using the systems development life cycle V-model as its framework. The first section, beginning with Chapter 2, is a discussion on risk-based ship design and roll the Wave Groups methodology plays in the quantifying risk for ship design and ship operations. Chapter 6 begins the

second section of the discussion, which represents the bulk of the thesis work. Here we discuss approach to the analysis and the steps taken to refine and validate the model. Chapter 4 provides details about the simulations setup and the design tools used for the analysis and Chapter 5 is the discussion on the simulation and analysis is presented in Chapter 6. The final section, in Chapter 7, is a discussion on the industry application of the Wave Groups methodology. This is presented in Chapter 7. Concluding remarks and considerations for future work are provided in Chapter 8.

Chapter 2

Risk Based Ship Design

In this section we discuss the development of risk-based standards in the maritime industry and highlight tools and methods designers have for risk-based decision making. Today, advances in computing tools have allowed designers to develop more detailed statistical and physics-based models to inform design decisions. Regulating bodies have traditionally lagged to keep up with advances in technology and knowledge. We define Risk as the product of event severity and event probability. This created two major areas of research quantification and prediction of extreme events. This is the foundation of the work presented in this study.

2.1 Historical Background

Most risk analysis approaches can be traced back to the nuclear industry, for which risk analysis became important in the 1960s. The goal was to calculate the probability of the release of nuclear contaminants. Decades later, the Piper Alpha disaster in 1988 forced the offshore industry into risk analysis as a requirement started with the Norwegian government and by the United Kingdom in 1992. Many more members of the Organization for Economic Co-operation and Development (OECD) soon followed [1].

Historically, in the maritime industry, regulations were a reaction to major accidents or disasters. In many cases, these regulations resulted from an ad hoc safety

assessment process seeking to reduce public and political pressures for action. Such processes favor quick solutions over a rigorous technical analysis that explores the cost versus benefits of solutions. Worse, this reactive approach has made the regulation system more complex as amendments are continually made, thus leaving limited room for innovation and advancement in the industry. Further analysis showed that this approach to safety standard was a symptom of prescriptive regulation, where the burdened of technical analysis laid on the regulating body and classification societies (e.g. IMO and the American Bureau of Shipping), leaving it up to ship builders to design within the prescribed constraints.

The transition to risk-based approaches began with probabilistic damage stability standards in the 1960s, but took decades to be introduced by the International Convention for the Safety of Life at Sea (SOLAS). SOLAS is responsible for setting the minimum safety standards for the construction and operations of merchant vessels. The International Maritime Organization (IMO) maintains and amends these standards, which, until 2009, were updated as a result to collision accidents and disasters. Project HARDER (1999 to 2003) investigated elements of the traditional approach and proposed a new formulation for the probabilistic damage stability employing enhanced computational models and statistical methods [6]. The final recommendations from this study were adopted in 2005, prompting a four-year study, Project SAFEDOR (Design, Operation and Regulation for Safety), across a consortium of fifty-two European organizations to incorporate risk-based approaches into ship design, operations, and regulations [1]. This effort concluded in 2009 when the regulations were entered into force at the IMO.

2.2 Risk-Based Ship Design

The maritime industry moved to risk analysis or risk-knowledge models as a proactive approach to safety standards to get ahead of future disasters and to improve innovation. The maritime industry, in one way or another, has been caught between two main design drivers: (1) economic drivers to push more cargo faster and cheaper;

and (2) societal drivers to reduce losses at sea and to do less harm to the environment. Under these pressures and limitations of traditional prescriptive regulations, ship designs quickly reached a sub-optimum optimal. Figure 2-1 illustrates the gap between prescriptive regulations and technical feasibility [1].

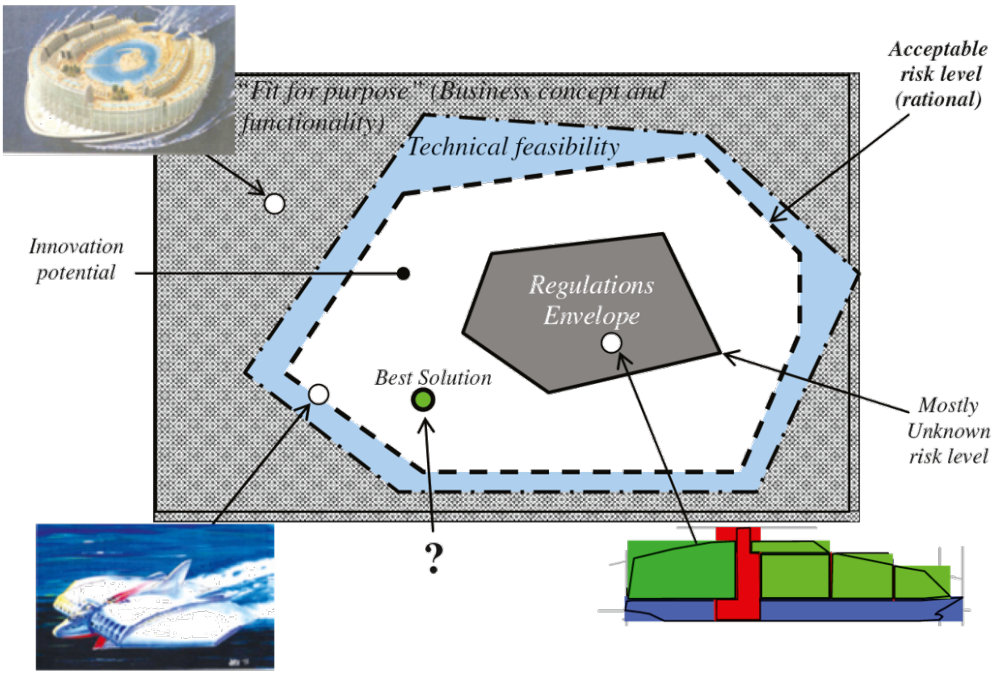

Figure 2-1. Possible design envelopes [1]

Risk based ship design offers two approaches to realizing the innovation potential that is the gap; safety equivalence, where the standard is based on a reference vessel or defined by a specified risk acceptance criterion [1]. Both approaches derive from the introduction of safety as an objective in the design process.

2.2.1 Risk-Based Design in the U.S. Navy

The United States Navy manages some of the world's most expensive portfolios of projects. The average cost of just one of the sixty-six active Arleigh Burke-class guided missile destroyers is upwards of $1.8B plus further cost for operation and support throughout the life of the ship. The process for the design and acquisition of projects of this scale are outlined in the Operations of the Defense Acquisition

System, more commonly known as the DoD 5000. Figure 2-2 depicts this Defense Acquisition Management Framework. The dotted red lines highlight where in the process the findings of this (and related studies) could be applied using risk-based models.

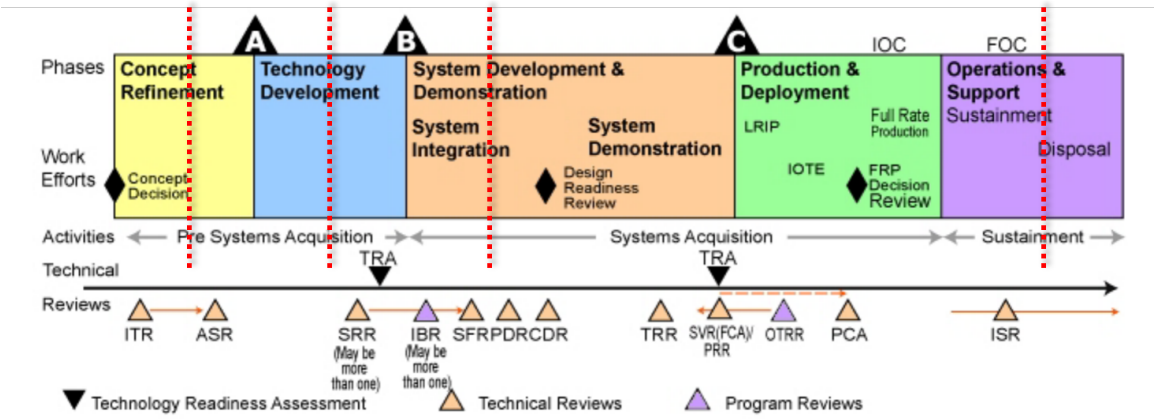

Figure 2-2. Defense Acquisition Management Framework [2]

When designing a ship or writing design specification and operating limits, designers and project managers must consider the worst reasonable situation. The main problem with these "worst" design situations is that they are very rare and difficult to quantify. Risk-based ship design offers a framework to understand the risk being accepted and the characteristics of these rare but catastrophic events. The complete process requires a combination of physics-based simulations, statistical methods, and model testing. During an interview at Naval Surface Warfare Center - Carderock Division (NSWCCD), engineers working in the maneuvering and seakeeping division agreed with our belief that no combination of these tools is mutually exclusive, rather a systematic application of all three should be the recommended approach.

2.2.2 Model Testing

Model testing has been a critical aspect of naval architecture since before the 20th century. Reynolds and Froude offer similitude principles that allow engineers to translate the physics of full-scale operations to a smaller scale and for much lower cost. The International Towing Tank Conference (ITTC), established in 1932, is

a non-government organization that has been charged with establishing standard practices for ship model work, procedures, and methods of result presentations. Today their aims include improving methods for, and recommending procedures for, physical model experiments, numerical modeling, full-scale measurement of ships and marine installations [7].

Data collected over the past century of model testing and accidents has created a vast wealth of knowledge, which has been used as the basis of computational models that allow designers to optimize about a set of design requirements. Mathematical models are traditionally used to fill the knowledge gaps for which testing was not or could not be accomplished, and to extrapolate to the far reaches of the design spaces that have yet to be explored. Though more economical than full-scale testing, model testing is still a slow, resource-exhaustive process that is ill suited for capturing statistics of rare events efficiently. At NSWCCD, Ken Weems shared that even after three hours of simulation, the mathematical fit may not be right. For instance, a Weibull fit for an extreme bending moment model may vary between a factor of two, or five in certain cases, dependent on the length of the simulation [8]. When operating on the tails, where extreme events reside, conditions change quickly and uncertainties have a large impact on the reliability of these models. The belief in this study, is that these models can be made more reliable by incorporating more deterministic simulations at the extreme cases that lead ship instability.

Naval architects face two main questions with model testing; (1) how to best replicate the real-world wave environment and (2), what are the most interesting conditions that are worth replicating? NSWCCD has gone to great lengths to address these questions directly. Originally built in 1962, the Maneuvering and Seakeeping (MASK) basin allowed engineers to test the performance of ships and moored systems in realistic sea conditions using pneumatic actuators. Figure 2-3 is a design drawing of the 86.400 ft^2 basin. In 2013, the facility completed a six-year renovation project to replace the original actuators with 216 individually controlled electro-mechanical wave boards. This allowed for greater capability and control of the wave generation process at high frequencies, and flexibility to customize the spectral shape and wave-front of

the wave systems. As a departure from the traditional tow-tank testing approach, very few facilities like this exist around the world that can evaluate maneuverability, stability, and control of models.

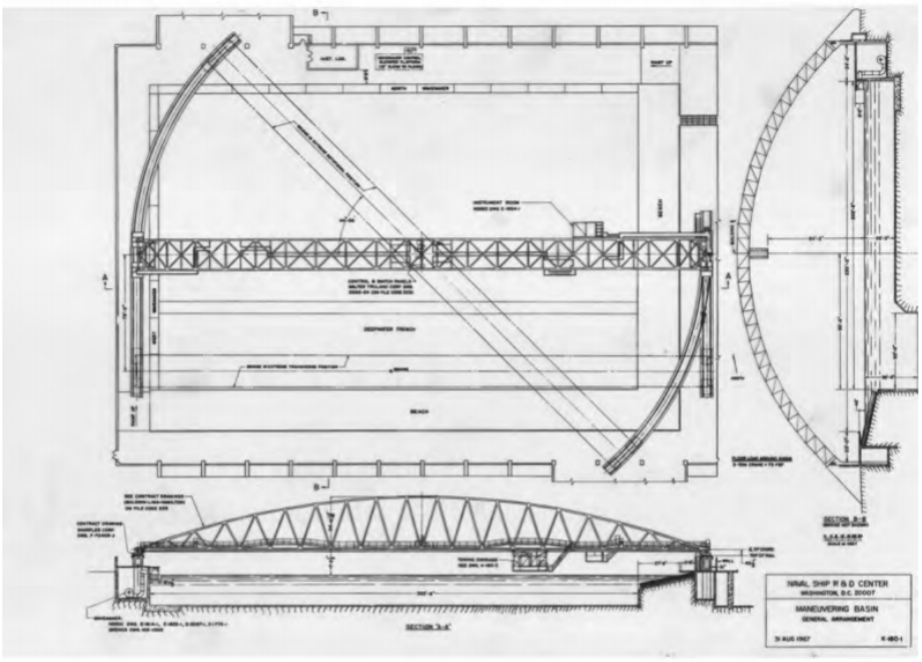

Figure 2-3. Historical Drawing of NSWCCD Maneuvering and Seakeeping Basin [3]

However, to fully characterize the extreme events that a vessel would encounter during its twenty-five-year service life, it would require years of model simulation and even longer to make a statistically relevant argument. Computer simulations offer a complementary solution to model testing, where by the simulation can be used to identify the few seaway characteristics and operating scenarios for engineers to replicate and study using model testing.

2.2.3 Computer Simulations

Computers simulation offer several alternatives to traditional model testing. Quantification of ship response statistics through transfer function analysis works well for the case of linear responses. Solving these problems in the frequency domain, the ship response calculations can be resolved with little computational effort [9]. These tools have helped the ship design industry to understand the core of the probability density

function (PDF). Though useful, this is not necessarily the limiting design case. The extreme response phenomenon lay in the tails of these PDFs. The non-linearities arise from interaction between the wave and hull geometry. Cousins and Sapsis, at MIT SAND lab, have shown that the frequency domain analysis does not sufficiently characterize the tail structure of ship roll response [10]. Instead, they noted that the extreme the roll events occur more commonly than predicted. Computational fluid dynamics (CFD) using potential flow models can reconcile these non-linear interactions and capture these response phenomena. Today, CFD tools substitute a significant portion of model testing, and in some cases, replace model testing altogether. Potential flow and strip theory provide resistance, stability, motions, and loading conditions [9]. To collect data on the short-term statistics for these parameters, naval and marine engineers have long used direct Monte Carlo simulation to reproduce realistic seaways in the computational environment. Monte Carlo is a robust approach, but has a major drawback; the accuracy for capturing long term statistics is directly proportional to length of the simulation. Since the input waves are selected directly from a wave power spectrum, the probability of a response event is coupled directly with the wave spectrum. On a standard PC, the pace of Monte Carlo simulation is just shy of being about real-time. This is too slow when the goal is to write a design specification or standards for an event that might occur a few times during the 25 year or longer service life of a vessel.

2.2.4 Quantification of Extreme Events

Since the IMO adopted RBSD as a regulatory framework, the maritime industry, including the US Navy, has gradually shifted to better quantify and predict rare and catastrophic events. The challenge with this approach, lies in modeling these systems of systems. In many cases, the physics we use are computationally demanding and the cost at stake continues to grow. Consider the Navy's risk related standards, where the requirement is that the ship should be designed for to survive and event that happens during 0.0001% of the life of a ship. With an average thirty-year service life of a US Navy warship, this equals approximately 200 to 1000 hours of operation [11].

The probability of a catastrophic event outside of this area is beyond the scope of the design. To observe such an event, the direct Monte Carlo approach would have to produce 500,000 hours of simulation. Further, to achieve the level of statistical significance, this event should be observed no less than 10 times, totaling 5,000,000 hours of simulations for a single combination of speed a heading. Quickly, the size of this analysis becomes insurmountable even for the most advanced computer clusters.

The alternative to capturing statistics of these extreme events is what we have mentioned already, extreme value theory (EVT) fit by mathematical models. The precept for EVT is that rare events are similar in their behavior based on some non-linear physical property. The second approach is the Wave Groups methodology. A wave group is a sequence of waves related by a function of amplitude, period, and length scale. The Wave Group methodology has been used in the past to deconstruct wave systems into discrete portions. We apply this methodology by capturing the deterministic ship response to each wave groups in a large set. By overlaying the probability that a ship will encounter the wave group, we are able to calculate the statistics of the response event itself. In practice, the EVT and Wave Groups methods are complimentary because they seek to solve the same problem using different sets of assumptions. for the case of our sponsors at NSWCCD, if both approaches can provide the same result, this makes the approval process for a future risk-based standard or model more palatable.

2.2.5 Model-Based Engineering in Ship Design

The purpose of running these computational simulations is to capture the short-term and long-term statistics of ship response parameters. This is part of the larger vision to quantify the frequency and severity of events to help understand risk for the design and decision-making process. Computational models offer endless application, from understanding complexity to streamlining the design process. Models also pose disadvantages. Relying on a model without understanding considering the uncertainties or limitations, can be just as bad as using a random number generator. In all cases these system engineering models seek to combine aspects of the physical state

with event probability and decisions to approximate a future system state and risks associated with those states.

Project SAFEDOR assembled design teams to tackle the following eight design scenarios using risk-based design approaches. In all scenarios, the teams developed several innovative tools using model-based system engineering to show how risk-based ship design could be incorporated into the design, decision making, operation, and regulation on the maritime industry. The impetus of the new design framework was for teams to balance performance and cost with a new objective - minimize risk [12]. Table 2.1 lists some of the unique applications of risk-based design that were accomplished during Project SAFEDOR.

1	Optimize a post-PANAMAX size cruise vessel based on new probabilistic damage requirements.
2	Design a cruise liner that will be safer than existing ones and reduces incidental damage to environment in case of grounding or collision.
3	Increase cargo capacity of an existing fast full-displacement RoPax ferry.
4	Design a RoPax ferry for 50 passengers using risk-based principles vice SOLAS requirements.
5	Develop a fire risk model to provide a quantitative measure of risk of new designs and economic benefit for a new lightweight composite superstructure.
6	Develop a short-sea LNG vessel to distribute gas using the safety equivalence of the CNG rules.
7	Develop a competitive, low-gross tonnage open-top container vessel using safety equivalence to overcome the current regulatory disadvantages.
8	Optimize a post-PANAMAX size cruise vessel based on new probabilistic damage requirements.
9	Multi-objective optimization of an AFRAMAX tanker by genetic algorithm to improve transport economy and reduce environmental impact.

Table 2.1. Applications of risk-based design explored during Project SAFEDOR

As the first large scale project to develop the risk-based regulatory framework for the maritime industry, the work provided first principle approaches to safety and

corresponding design tools. During the early stage design, tools for risk analysis could be simpler (e.g. expert judgments, databases, or simplified formulas). As projects progress in to the concept and detailed design phases, these tools must become more rigorous and verifiable [1]. Tools such as model-based system engineering and agent-based modeling have proven to be able to quantify safety as a measurable objective.

2.3 Wave Groups

This study applies the concept of wave groups for the quantification of risk in ship operation and ship design. The basis of this formulation, also known as critical wave groups, is that probability of a certain type of ship instability may be determined by the probability of encountering the wave group that generated that instability. This approach disassembles the problem in to a deterministic and a probabilistic part [13]. This decomposition-recomposition of the problem shown in figure 2-4 is intended to deal with the non-linearity.

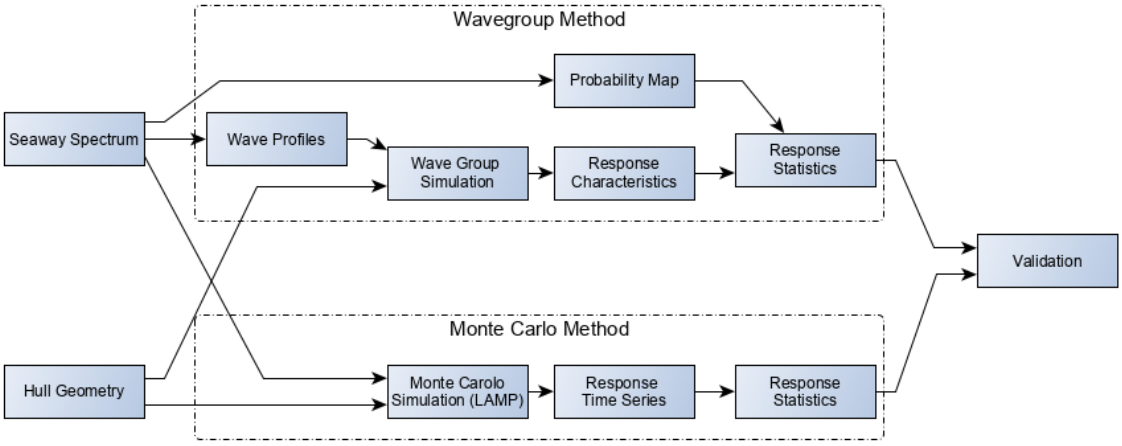

Figure 2-4. Wave group process using decomposition-recomposition approach

Wave groups have been the focus of much of the work motivated by risk-based ship design and risk-related standards. Previous work completed by Anastopoulos et al, identified wave group characteristics such as height, period, and length scale through the deterministic evaluation of ship dynamics. A Markov chain model was used to capture probabilistic part by determining the frequency of encountering any

wave group above a certain threshold [13]. The principal focus of this study was to construct wind-generated, high probability wave groups and used them for the assessment of ship stability in irregular seas.

The pitfall is that quantification of the wave groups must be consistent with the physical mechanisms of the response. Previous work has shown that if we propose an arbitrary non-linear response that was only based upon wave elevation, the approach may work well to capture some of the response parameters, but is unable to capture others. Essentially, the problem is more complicated and the wave slope or the distribution of the waves over space must be consistent to capture all response parameters.

2.4 A Regulatory Perspective

The IMO is responsible for publishing stability standards for all vessels. These standards provide a general framework for designers. With the focus on safety, these guidelines often fall short of maximizing performance and accounting for extreme events.

The rapid pace of technology has brought on design tools and manufacturing methods with which traditional prescriptive standards have struggled to adapt. The 2008 Intact Stability Code published by IMO was the first acknowledgement from a standards or classification body that design technology is rapidly evolving and codes should be re-evaluated and revised as necessary. The code further recognized many of the challenges with the quantification of extreme events that have been discussed, specifically that "complex hydrodynamic phenomena have not yet been fully investigated and understood" [14]. This was a significant shift from the retroactive approach to a model-based approach.

Chapter 5.1.1 of the IS Code explicitly states that "compliance with the stability criterion does not ensure immunity against capsizing, regardless of circumstances" [14]. Though understandable, this is a bold statement from the organization responsible for setting standards for stability and safety at sea. The problem of quan-

tifying the risk due to extreme events at sea remains a challenge that many around the globe are actively working to address. The approaches and methods discussed in this study represents a novel approach towards this problem.

Chapter 3

Theoretical Analysis

In principal, we know that the formulation of the wave system does not a priori consider the formulation of the ship response. Potential flow simulation was used to capture the response motion and loading conditions deterministically for both the control and wave group experiments. The control data was developed using direct Monte Carlo simulation during previous work completed by Stevens [15]. During his work, Stevens characterized an original set of wave groups by modulating peak amplitude and length scale. Over the course of this study, we sought to characterize the slope of the incident wave group. A brief overview of the direct quantification and wave group implementation is discussed followed by two numerical approaches that were implemented for the experimental set.

3.1 Direct Quantification

Direct Monte Carlo simulation is one method for reconstructing wave fields from a wave power-spectrum. Wave-power spectra differ by regions of the world and are developed through extensive data collection over several years of observation and experimentation. To implement Monte Carlo, the wave spectrum can be divided into equally n-integer subdivisions. The simulation randomly selects the average frequency over the subdivision limits based on the probability of occurrence. The wave elevation of the resulting linear waves can be superimposed over space and time to produce a

realistic seaway using 3.1. An example of the resulting 1-D wave system is shown in figure 3-1.

$$\zeta(x, y, t) = \sum_{n=1}^{N} A_n \cos(k_n(x \cos \beta_n + y \sin \beta_n) - \omega_n t + \theta_n) \tag{3.1}$$

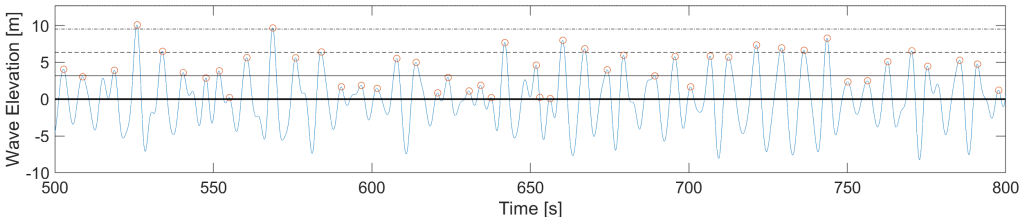

Figure 3-1. Wave system developed using Monte Carlo

A	peak wave group amplitude	β	wave heading
ω	peak frequency	θ	phase angle
L	length of the wave group	k	wave number

In equation 3.1, ζ is total wave elevation sum of the linear waves generated by the wave-power spectrum. It is generally accepted that the wave elevation of a seaway is a stationary ergodic, Gaussian random process [16]. The ocean waves we are most interested to reproduce are wind generated wave described by the JONSWAP spectrum. More details on the spectrum used for the simulation are provided in 4. In summary, the JONSWAP spectrum is narrow banded, as such the wave elevation follows a normal distribution and the probability distribution of the peaks can be defined by a Rayleigh distribution, 3.2.

$$f_{peaksofh}(\alpha) = \frac{\alpha}{(\alpha_h)^2} \exp^{-\frac{\sigma^2}{(\sigma_h)^2}} \tag{3.2}$$

3.2 Wave Group Decomposition

The Wave Groups methodology considers the analytical decomposition of a random wave field into short, discrete wave groups. The assumption of a hyperbolic-

secant-shaped profile was selected following work completed by Sapsis and Cousins [10]. The resultant windowing function $\eta = A(t)sech(\frac{x}{L})$, shown in figure 3-2, was implemented to produce the modified wave elevation equation, 3.3, [15].

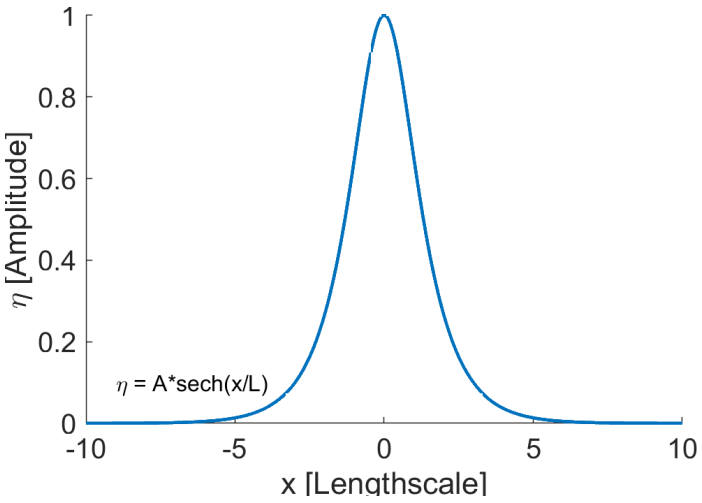

Figure 3-2. Discontinuity in time series data

$$\eta(x, y, t) = Asech(\frac{x}{L})\cos(k(x\cos\beta + y\sin\beta) - \omega t + \theta) \tag{3.3}$$

In equation 3.3, we consider a single wave system, whose elevation is $\eta(t)$. The wave number is defined by the dispersion relationship for deep water waves, equation 3.4, where g is gravity, and λ is the wavelength.

$$k = \frac{2\pi}{\lambda} = \frac{\omega^2}{g} \tag{3.4}$$

The key advantage of the wave groups, is that it can be completely determined by a few parameters and the realistic range of these parameters is determined by the record we collected from the long Monte Carlo simulation. Figure 3-3 is the resulting wave system with the windowing function in red, shown along the peaks of the wave.

3.2.1 Wave Group by Length Scale

The first implementation of wave group sampling was developed using the joint probability of length scale and amplitude [15]. This worked well to capture some

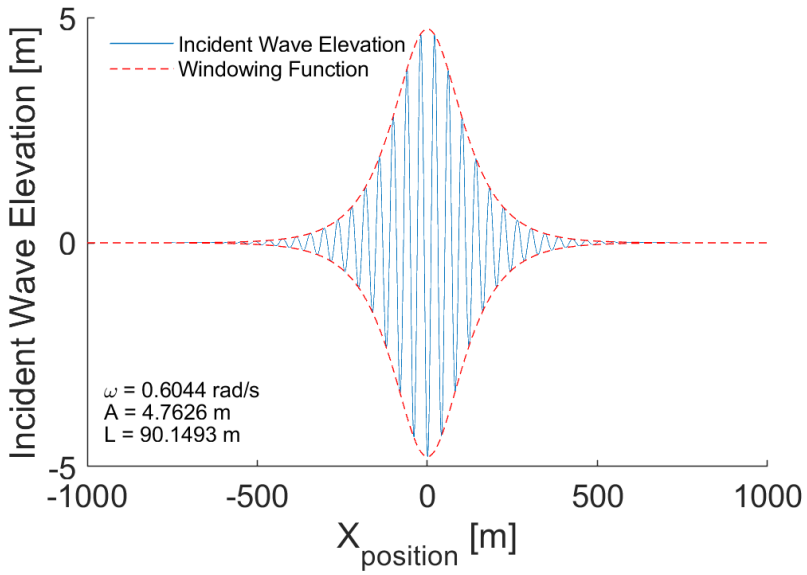

H]

Figure 3-3. Incident wave system generated by modified LAMP

response parameters, F_x minima, F_z maxima and minima, but fell short in cases of pitch maxima and minima, F_x maxima, and M_y maxima and minima. Further inspection suggested the quantification of these wave groups was not consistent with the physical mechanisms of the response and that the problem was more complicated.

wave groups reconstructed in figure 3-4 show the wave elevations of two such sampled wave groups. Here the peak frequency is constant and the peak amplitudes were nearly identical. However, the slope of the wave was not properly characterized ($blue = 2.878$ and $red = 3.191$).

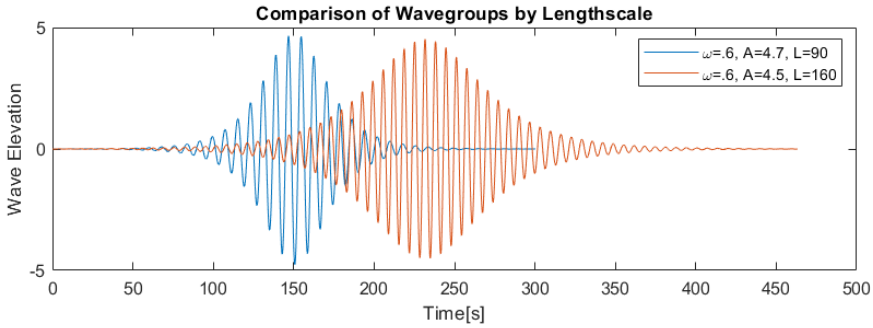

Figure 3-4. Wave Elevation Comparison

Figure 3-5 shows the resulting surge force, F_x, response. The peak response is dramatically different between these two wave groups. The peak force for the 90m

wave group is nearly five times larger than the 160m wave group for the same amplitude. The slope of the wave is a key driver in the formulation of the ship response and was not a controlled parameter from this first sampling set.

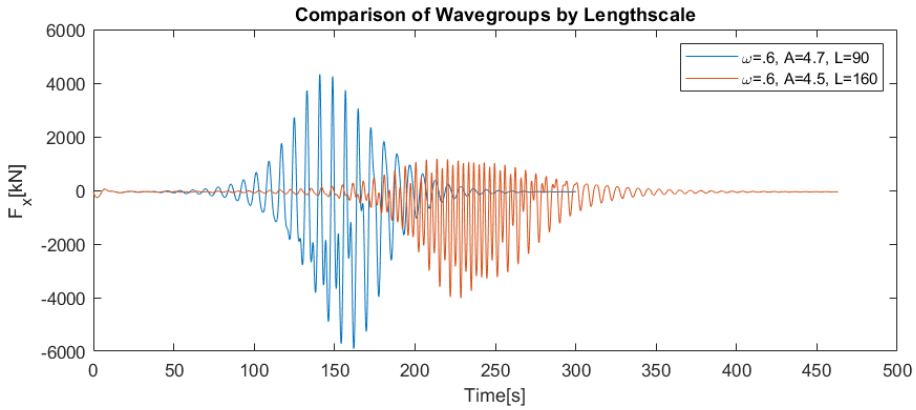

Figure 3-5. Wave Elevation Comparison

3.3 Capturing the Slope

From the example shown above, we knew that the wave slope needed to be an input in the form of probability distribution rather than a product of the windowing function. However, we were limited in the inputs that we could give LAMP to L, A, ω_o, x, and ϕ. To extract the frequency from the time series data, we considered a simplified, 1-D, wave system with a random phase angle, $\theta = [0 : 2\pi]$. This simplified the incident elevation equation for the wave groups to 3.5.

$$\eta(x, y, t) = Asech(\frac{x}{L})\cos(kx - \omega t + \theta) \tag{3.5}$$

The gradient of the η with respect to time is the slope of the time series 3.6.

$$\frac{d\eta(x,t)}{dt} = \omega Asech(\frac{x}{L})\sin(kx - \omega t) \tag{3.6}$$

If we consider the slope and elevation to be independent variables, we can use their product to develop a joint distribution map. From this we can calculate the

frequency, ω, for individual wave groups using the approach in 3.7.

$$\frac{\eta'}{\eta} = \frac{max[\omega A sech(\frac{x}{L})\sin(kx - \omega t)]}{max[A sech(\frac{x}{L})\cos(kx - \omega t)]} \tag{3.7}$$

The hyperbolic secant and amplitudes canceled, and the maximum value of one for both sine and cosine, also canceled. The remainder was the frequency with units of radians per second.

$$\frac{\eta'}{\eta} = \omega \tag{3.8}$$

The co-variance of the one million data point set of slope and amplitude was 0.85. However, after considering multiple smaller sets, we found that the co-variance failed to converge to a single value, in other words, what we were observed was just noise. This was enough to conclude that slope and elevation were indeed independent sets. This was made simpler because both the wave elevation and its derivative followed Rayleigh distributions, as expected.

$$f_{peaksofh}(\alpha) = \frac{\alpha}{(\alpha_h)^2}\exp^{-\frac{\sigma^2}{(\sigma_h)^2}} \text{ where, } S_{h'h'} = \omega^2 S_{hh} \tag{3.9}$$

$$f_{peaksofh'}(\alpha) = \frac{\alpha}{(\alpha_{h'})^2}\exp^{-\frac{\sigma^2}{(\sigma_{h'})^2}} \text{ where } \sigma_{h'}^2 = \int_0^\infty S_{h'h'}(\omega) \tag{3.10}$$

After normalizing each distribution to one, we can calculate the joint probability density function as the product of the two distributions.

$$f_{h,h'}(\theta_1, \theta_2) = f_{h'}(\theta_1) \cdot f_h(\theta_2) \tag{3.11}$$

Chapter 4

Experiment Setup

This chapter describes the major components of the experiment, to include the simulation software, the hull geometry, and the input seaway characteristics.

4.1 Simulation Tool

4.1.1 Large Amplitude Motions Program (LAMP)

This study primarily used the Large Amplitude Motions Program (LAMP) to simulate the wave-body interaction problem. Developed in 1989 by the Science Applications International Corporation (SAIC) and later, the Leidos Corporation, LAMP calculates time-domain motions and loads for floating bodies using 3-D potential-flow panel method and viscous effects are included as an external, non-pressure forces in the overall force calculation. The challenge with any physics-based formulation that incorporates nonlinear wave-body interaction is in balancing the computation requirements with correctness and complexity. To do this, LAMP offers the user multiple options for the complexity of calculations.

- LAMP-1: Body-linearized 3-D
- LAMP-2: Approximates large-amplitude 3-D body-nonlinear method with assuming steady forward speed

- LAMP-3: Approximates large-amplitude 3-D body-nonlinear method allowing large lateral motions

- LAMP-4: Large-amplitude 3-D body nonlinear method

The LAMP-2 method sufficiently captured the body nonlinear effects for this study with slightly more computer resources than LAMP-1. This method used the body-linear 3-D approach to compute the hydrodynamic part of the pressure forces, while the nonlinear hydrostatic restoring and Froude-Krylov wave forces were calculated on the actual hull surface below the incident wave surface. The very important aspect of the time-domain approach implemented in LAMP is that it provides and event-driven analysis of the ship response to a specific wave event rather than a general statistical solution of the ship motion problem.

4.1.2 LAMP System

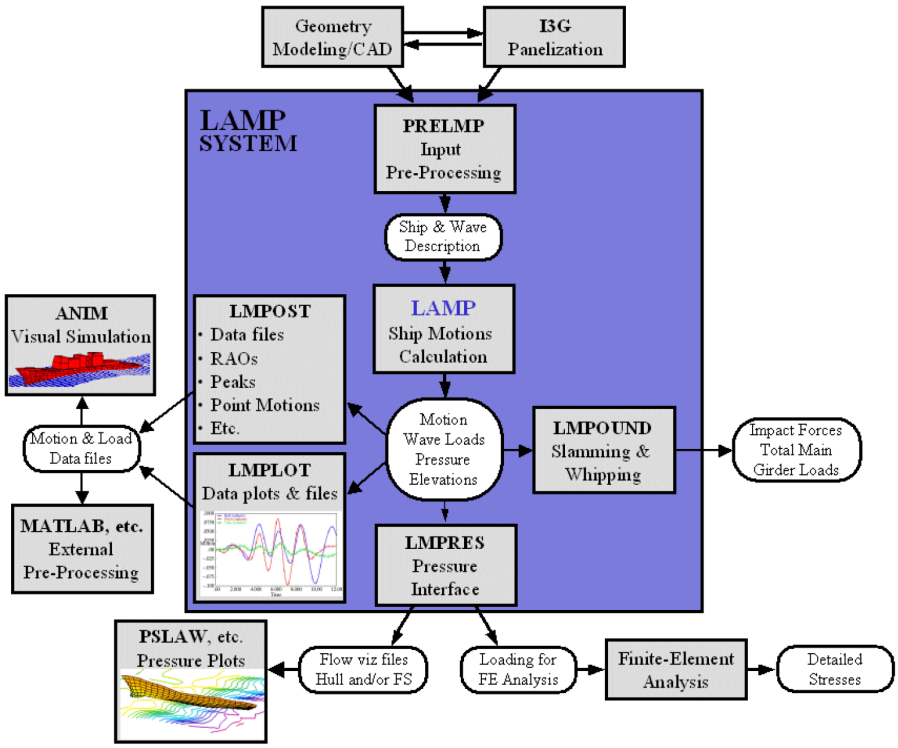

Figure 4-1. Structure of LAMP-Based Analysis System

The LAMP System is a comprehensive suite of software tools that include pre-processing, hydrodynamic calculations, general data processing, flow visualization, and finite-element structural analysis. Figure 4-1 from the LAMP manual explains the structure of a LAMP-based analysis.

This study used LAMP for direct Monte Carlo simulation as well as the wave groups sampling experiments. Previous work by Stevens developed MATLAB code that automated the process of generating input files, executing LAMP simulations, and parsing the output data for statistical analysis [15]. This study improved upon this process by providing more tools to stream line the process while implementing additional methods of characterizing wave groups. Figure 4-2 illustrates the implementation of the LAMP system and MATLAB for this work.

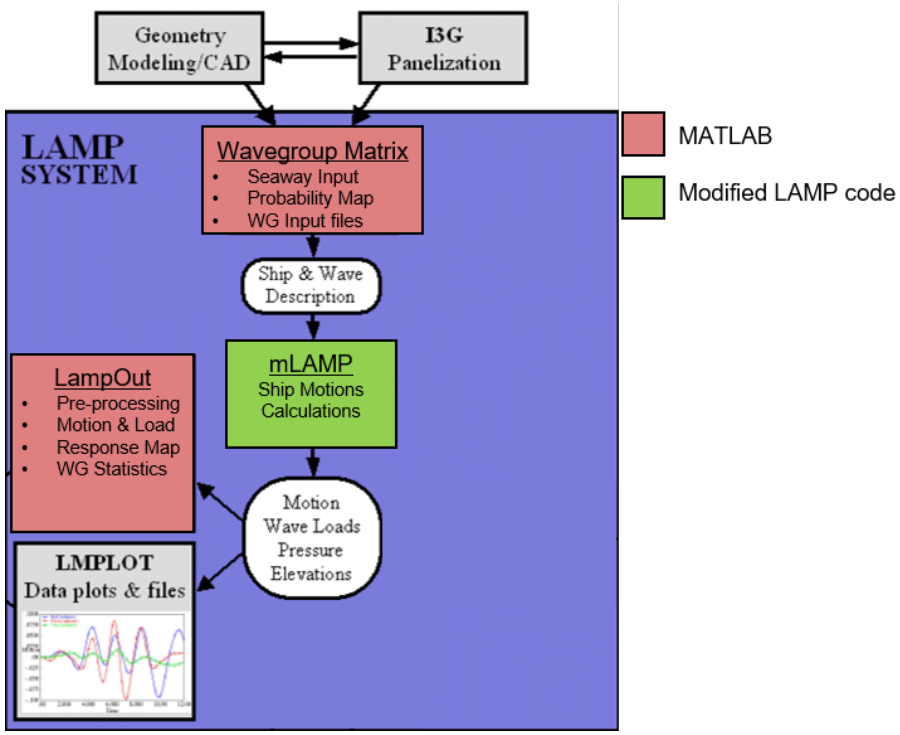

Figure 4-2. Implementation of LAMP and MATLAB for this study.

4.1.3 Modified LAMP

The original LAMP source code as adapted to accommodate the Wave Groups methodology discussed in 3. An explanation of the modification is provided in

Appendix A. This new version, which has come to be known as Modified LAMP (mLAMP), was developed Stevens while at MIT SAND lab [15]. Modified LAMP allowed us to completely define the wave group with three variables, frequency, amplitude, and length scale.

4.2 Input hull characteristics

One advantage of LAMP's 3-D physics-based formulation is that can accept both conventional and multihull structures. The formulation, however, is intended for displacement hulls and is not suitable for planing or surface effect ships. In coordination with on-going work MIT SAND Lab, we selected the ONR tumblehome hull for which the geometry and wave groups data that was readily available. The model was detailed enough to have research value, but was not representative of any U.S. Navy hull in service, allowing the results of this study to be released to the public.

The ONR tumblehome hull is representative of ocean-going naval surface combatant vessels. The tumblehome characteristic was most recently seen in the US Navy's *Zumwalt*-class destroyer. Advantages of this hull include superior radar signature reduction, as well as improved acoustics due to the reduced wake from the wave piercing bow. A primary disadvantage of this hull, and the reason it has been a topic of study, is the decreasing waterplane area due to the inward sloping freeboard. Table 4.1 lists the specific hull characteristics for this hull.

Characteristics	**Value**
LBP	154 m
Beam	18.78 m
Draft	5.49 m
Depth	14.5 m
Displacement	8507 t
Block Coefficient	0.535

Table 4.1. ONR Tumblehome hull characteristics

LAMP's graphics-based utility program, LMPLOT, was used to generate three-dimensional renderings of the input hull. Figure 4-3 shows the ONR tumblehome hull that was used for this study.

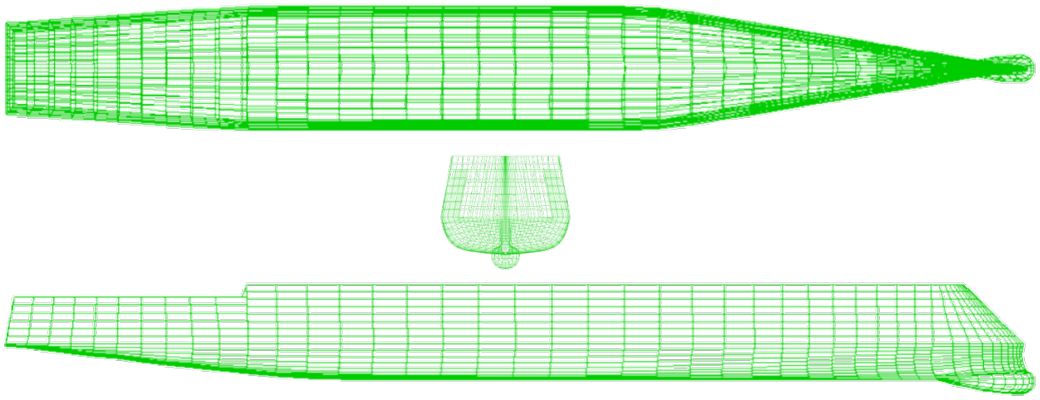

Figure 4-3. ONR tumblehome hull views

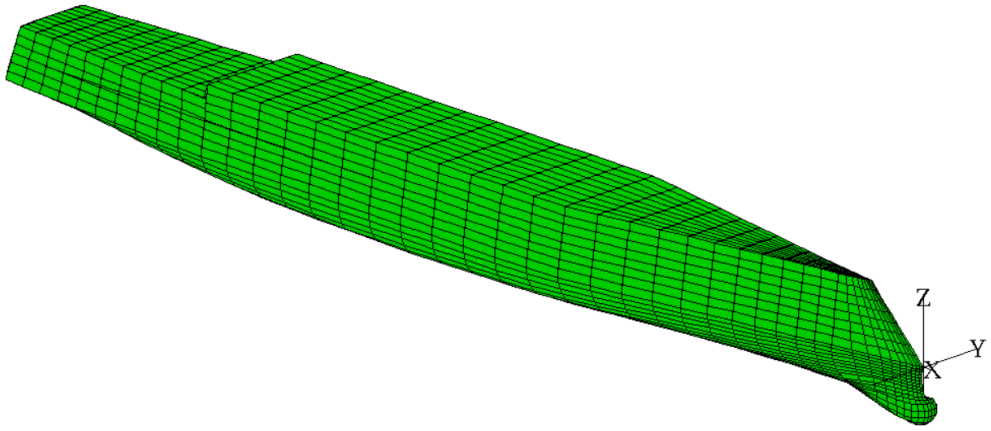

Figure 4-4. ONR tumblehome isometric 3-D view

4.3 Input seaway characteristics

Wind-generated ocean wave systems are best characterized by their power-spectral density functions. LAMP can reproduce seven input seaways: no seaway, multiple linear waves superimposed, a single non-linear Stokes wave, a long-crested 2nd order irregular Stokes wave, the Brettschneider spectrum, the Pierson-Moskowitz spectrum, the JONSWAP spectrum and the Ochi spectrum [17].

It was appropriate to continue to use the Joint North Sea Wave Observation Project (JONSWAP) ocean-wave spectrum to validate the new Wave Groups method-

ology against previous work [18] [15]. The JONSWAP spectrum was originally selected for its well-studied, irregular ocean spectrum. It accounts for non-linear wave-to-wave interactions that make it a suitable spectrum of long-term statistical analysis [16]. The LAMP expression for the JONSWAP spectral density is:

$$S^{+}(f) = \frac{\alpha g^2}{\gamma^5} \exp \frac{-5}{4} (\frac{\omega_m}{\omega})^4 \gamma^{\exp \frac{-(\omega-\omega_m)^2}{2\delta^2\omega_m^2}}. \tag{4.1}$$

$$\omega_m = 2\pi f_p \text{ the peak frequency}$$
$$\delta = 0.07 for f \leq f_p$$
$$\delta = 0.09 for f > f_p$$

The LAMP input parameters for JONSWAP are: fetch (γ), significant wave height(H_s), and modal period (ω_m). To effectively compare the results of this study with work completed by Stevens, the JONSWAP parameters remained unchanged between the two works. The resulting spectral density plot is displayed in 4-5.

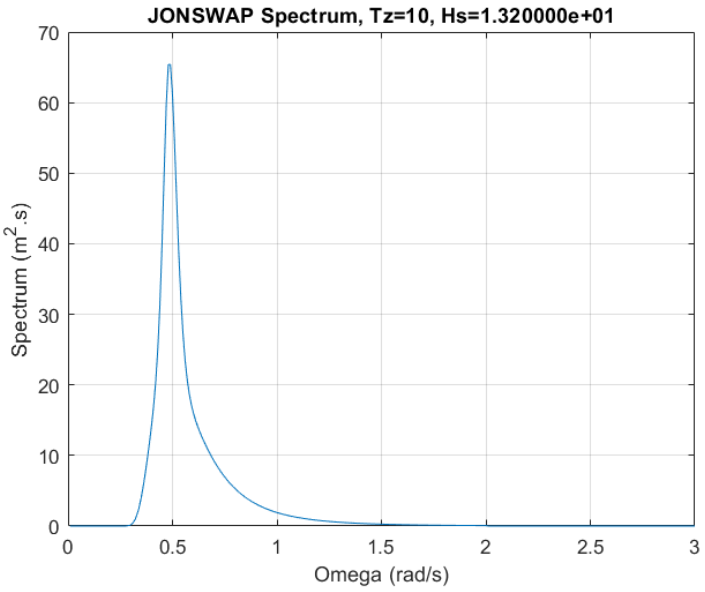

Figure 4-5. LAMP input JONSWAP spectrum

JONSWAP Spectrum: $\alpha = 0.060, \gamma = 3.0, H_s = 13.2\,\text{m},$ and $T_p = 10\,\text{sec}.$

The long time-series wave elevation closely followed a Rayleigh distribution as

expected 4-6

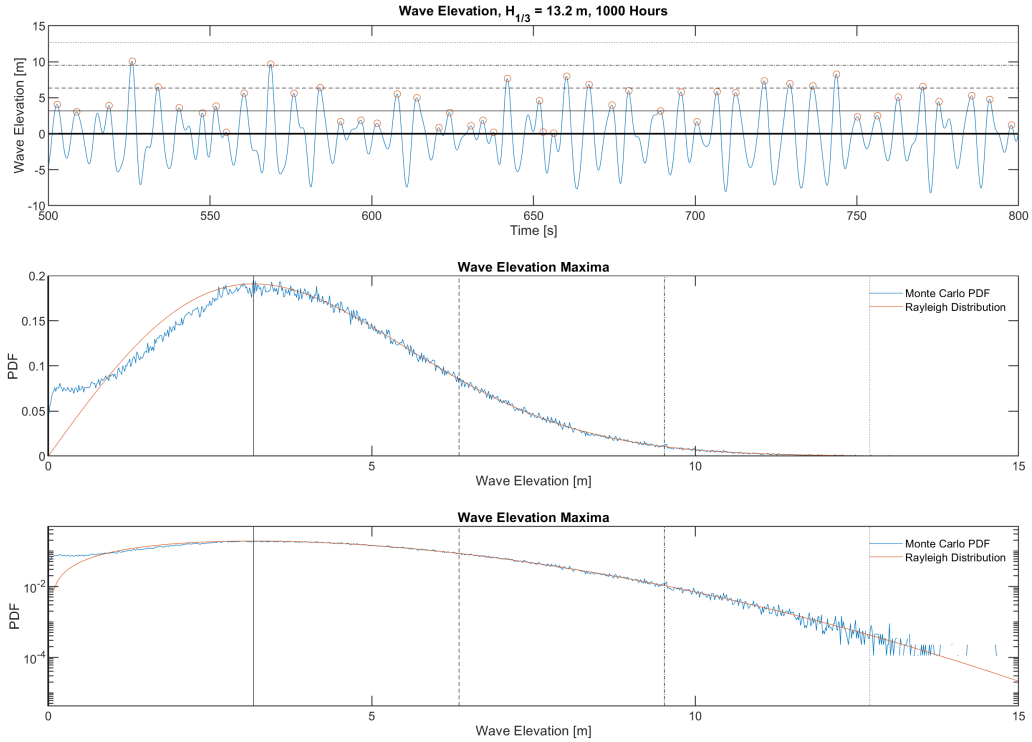

Figure 4-6. Wave Elevation Statistics

4.3.1 Data Corrections

A MATLAB script was used to count the wave peaks that followed mean up-crossings and the maximum slope in of the peak. These peaks are marked by a red circle and were used to develop the wave elevation maxima PDF. Nearly 8% of peaks occurred between -1 m to 1 m. In these cases, it was difficult to reconcile the incident frequency with the approach discussed in Chapter 3, resulting in frequencies that were abnormally large relative to the realistic waves systems. Moving forward, we considered only peaks whose elevation was greater than 1m and noticed little change to the wave elevation PDF.

To obtain the 1000-hour time series, 2000 30-minute LAMP simulations were concatenated. This was necessary to avoid self-repeating wave systems which is a known limitation of LAMP [15]. Each LAMP simulation also contained start-up and stop transients that skew the ships motions and loads. The start-up transient

ramps all wave elevations between factors of 0.0 and 1.0 over the first 120 simulation time-steps. When processing the data, the first 300 time-steps and the last 100 time-steps were removed to ensure accurate results. However, this method introduced discontinuities into the time-series data that needed to be accounted for in wave slope calculations, figure 4-7.

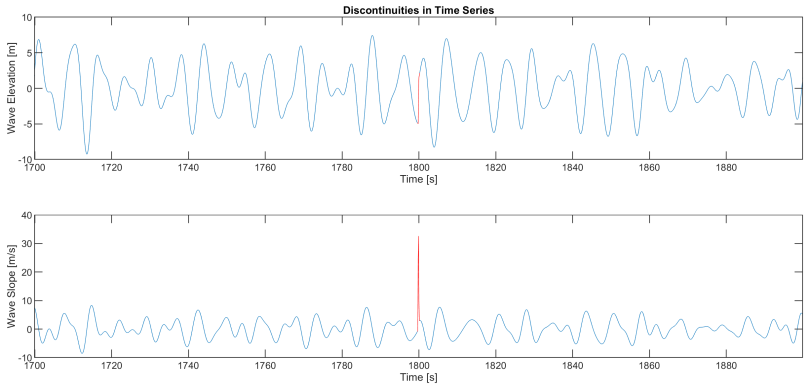

Figure 4-7. Discontinuity in time series data

Reproducing the time series data without discontinuities was possible, but is outside the scope of this work. The alternate solution was to exclude all slopes that exceeded 13.8, which is 0.003% (1099 points out of 3.5 million). The slope cutoff of 13.8 was chosen because it coincided with the point where Monte Carlo PDF diverged from the Rayleigh distribution, figure 4-8.

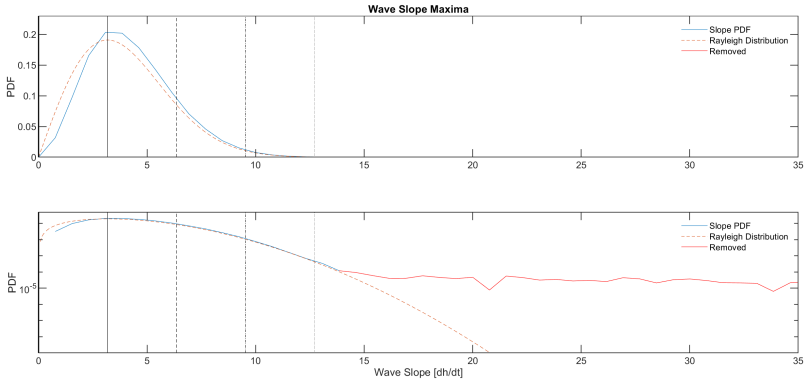

Figure 4-8. Monte Carlo wave slope PDF

The Rayleigh distribution verified that the peak slopes were representative of a physical wave system since we know the derivative of a Gaussian process, should also

be Gaussian.

4.3.2 Generating Probability Maps

We started with the probability map of the previously discussed JONSWAP spectrum that Stevens used to produce the wave groups of various amplitudes and length scales, figure 4-9 (left). Even though we shifted to a new approach, it was still necessary to establish an input length scale for the wave group. Figure 4-9 (right) shows the surge force response for these wave groups [15]. We noticed that force was relatively constant for θ_1 greater than 2 or 45 m. The value of $k_0 = 0.0402$, from the 10 sec peak period.

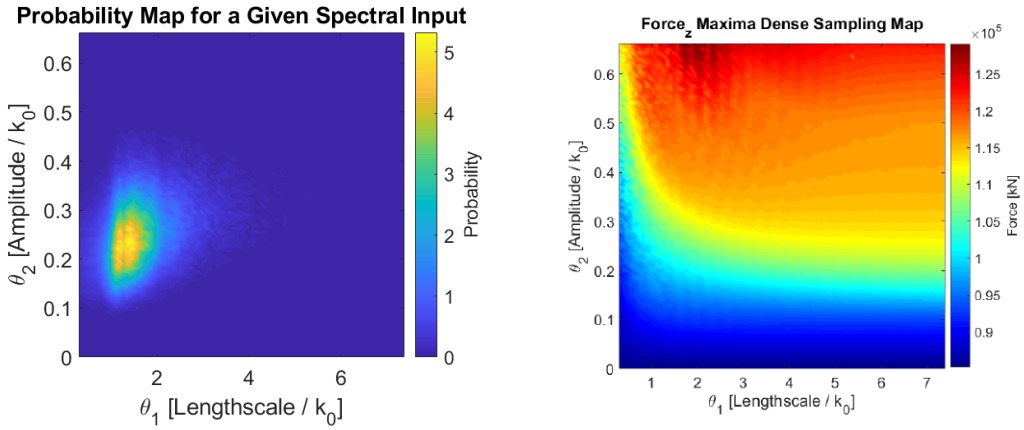

Figure 4-9. (Left) Length-Amplitude Probability Map. (right) Surge Maxima Response Map

This phenomenon occurred in all response cases which allowed us to choose a single length scale value of 3.6 or 90 m. This length scale was long enough to reduce variability in the results and short enough to keep simulation run-time as low as possible. By selecting a single length scale, we were able to maintain the two degrees of freedom analysis and maintain the simplicity of the problem.

Figure 4-10 shows the final distribution of the slope of the peaks and the joint probability map of the slope and peak amplitude. The probability map was combined with the wave groups sampling simulations to produce response maps and response distributions.

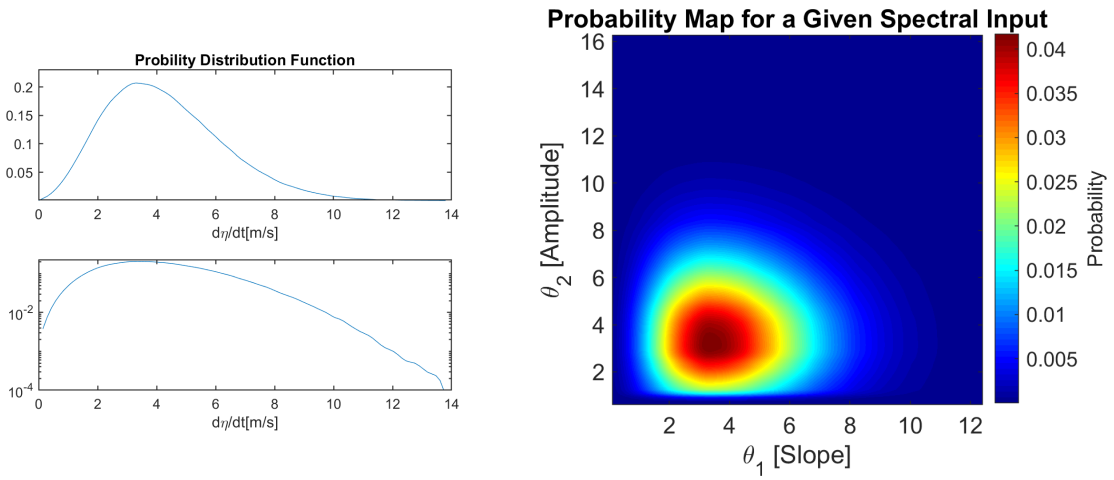

Figure 4-10. (Left) Wave slope ($d\eta/dt$) PDF. (right) Slope-Amplitude Probability Map

4.4 MATLAB Analysis

The LAMP systems offered an extensive suite of tools to generate and evaluate large sets of simulations. However, given the duration of this study, MATLAB provided considerable capability with a much smaller learning curve. Also, this work was built on previous work completed by Stevens and Mohamad who had also developed many tools in MATLAB for pre- and post-processing LAMP simulations.

4.4.1 Wave Groups Pre- and Post-Processing

As previously mentioned, the work completed by Stevens [15] provided data for 1000 hours of simulation. He used MATLAB to prepare, execute, and concatenate the short-time series results to produce this data set. From this set we were able to generate the probability maps using the procedures discussed in Chapter 3 for the wave groups analysis.

This study developed adapted versions of these tools to generate distributions for the wave slopes and frequencies that fed into the wave group simulation. A major portion of this work also included optimizing and streamlining these tools to provide greater functionality and be robust to user error.

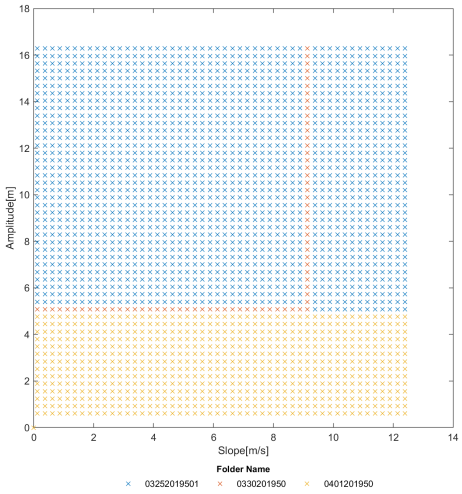

Figure 4-11. Progress plot output

4.4.2 Wave Simulation and Analysis Tools

During the development and testing of the simulation and analysis methods, it became quickly apparent that validating a large set of wave groups would be a monotonous ordeal. The sampling sets grow as the square of the sampling density. As we sought high resolution, the sampling density grew to 25, and later 50, restarting a 74-hour simulation after 50 hours was not sustainable. Additionally, as part of the quality assurance and understanding of the simulations it was necessary to filter and select interesting cases to animate.

The first tool develop was a simple script, *ProgressPlot.m* to read the files in the LAMP output directories to check for completed simulations. The script provides the user with a plot of completed wave groups by folder, 4-11. With this knowledge, a new set simulation could be started where the previous one finished (allowing gaps to be readily filled along the way). Furthermore, having the flexibility of knowing where each simulation resided allowed us to divide the simulations over multiple directories preventing corruption or total loss of a large set.

We found a simple solution in the analysis method. Since we were already using the wave groups to generate a response map for motions and loading conditions of interest, we could use resulting response maps as an interface to select the points that most stood out from the sampling set. The *ResponseMap.m* function gave the

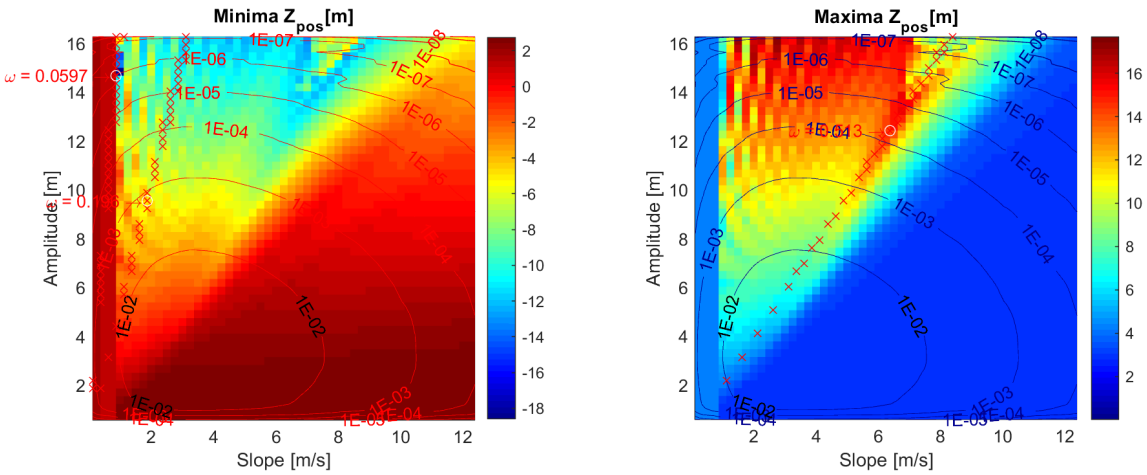

Figure 4-12. Selection of a single sampling simulation using the *ResponseMap.m* function.

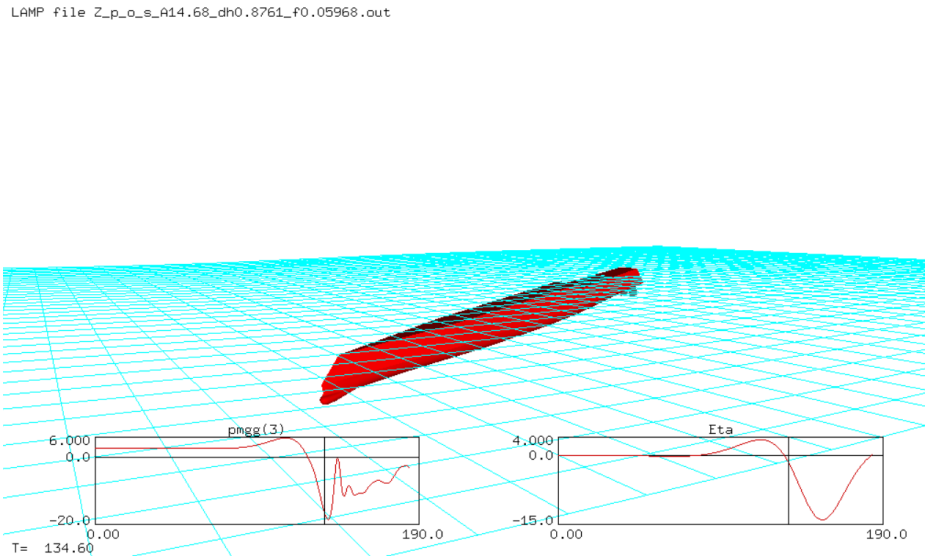

Figure 4-13. LMPLOT simulation of selected wave group sample

user the option to select a point on the response map of interested, which would be copied into a separate directory for further study. A white circle indicates the selected simulation and the red crosses indicated lines of constant frequency. Figure 4-12 is an example of an application of this click function.

The screen capture of the resulting simulation shows the failure of this LAMP simulation. This result was subsequently removed from the sampling space, Figure 4-13.

4.5 Response PDF Computation

Once the wave group sampling set was completed, we manually consolidated the output files into a single directory. The *LAMPOut.m* script removed the start-stop transients from each response time series, figure 4-14 and selected the maximum and minimum value, figure 4-15.

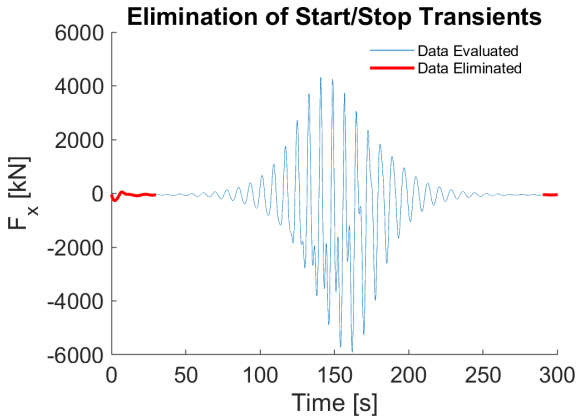

Figure 4-14. Processing LAMP transients

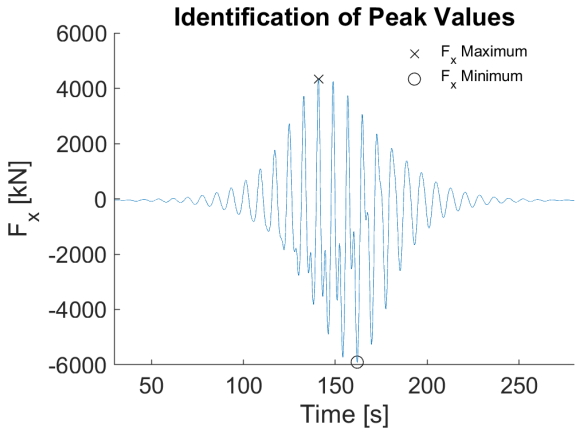

Figure 4-15. Wave Group max & min

These values were stored in an n-by-n matrix to produce simulation response maps. Once each simulation was processed, the script combined the wave group probability map and the response map to produce the response distributions. Chapter 5 discusses the simulations performance in more detail.

Chapter 5

Wave Group Simulations

5.1 Computational Tools

Fast computational performance has been a prerequisite to achieve practical application of simulating a hydrodynamic environment. Much of the work at MIT SAND lab has been to find new and innovative ways of reducing this computational cost. Although computational time depends largely the machine being used, the times recorded provide a representative view of the current performance achieved in an academic environment. All LAMP simulations and data processing was completed on a single desktop PC, Intel Core i7-3770 at 3.40 GHz, 16 GB RAM.

5.2 Simulation Performance

Early simulations attempted were run with as few wave groups across the probability map as possible. The since size of the wave group sampling set grows by the square of the number of samples across each distribution. The lower resolution sets, proved the simulations ran, but did not adequately produce reliable distribution curves of the ship response and loading conditions. Table 5.1 shows how the computational time changed with simulation size.

Sampling Density	3	5	10	15	25	50
Number of Wave groups	9	25	100	225	625	2500
LAMP Simulation Time [hrs.]	0.27	0.75	3.0	6.7	18.6	74.3
Data Processing Time [min]	0.21	1.0	2.4	5.3	14.8	59.8

Table 5.1. Simulation Summary

By evaluating the full range of amplitudes and slope distributions, we were able to update probability maps independent from the modified LAMP simulations. The LAMP simulations made up the 96% of the 78 hours of the computational time. The time spent reprocessing response for a new probability map was a fraction of the total time, table 5.1. The sampling size of 50 provided enough resolution to produce a smooth distribution for the response analysis. Previous work by Stevens showed that a greater sampling density provided little to no improvement in results [15].

5.3 Simulation Outputs

5.3.1 Motion and Loading Response

Figure 5-1 is a short time series set of all the response parameters from the original Monte Carlo simulation. By simulating wave groups that approached directly off the bow, we were able to simplify the analysis from 12 response parameters to five, table 5.2. All values were calculated about the ship's center of gravity (CG). Evaluating motions caused by beam or quartering seas was outside the scope of this study and has been left for future work.

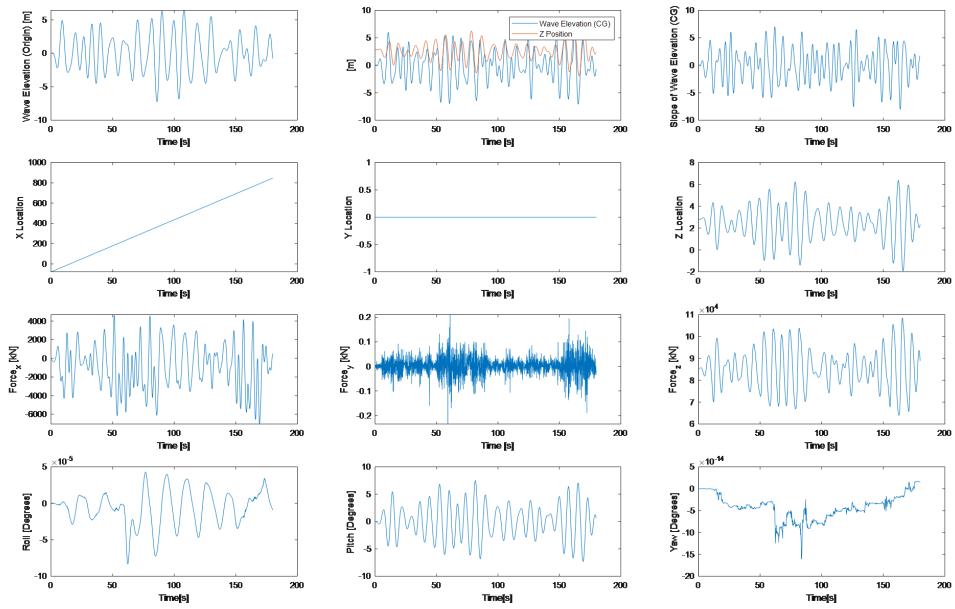

Figure 5-1. Time series summary of response parameters

1	Vertical position of CG $[Z_{pos}]$
2	Surge force at CG $[F_x]$
3	Heave Force at CG $[F_z]$
4	Pitch about CG $[Y_{rot}]$
4	Pitching Moment about CG $[M_y]$

Table 5.2. Response Parameters of Interest

5.3.2 Failed Simulations

Figure 5-2 is the run time for each slope-amplitude wave group simulation. By tracking simulation time, we learned that run time was a good proxy for simulation performance. The average simulation processing time was 107 seconds, so simulations that ran for less than 70 seconds, ended early because of a capsize or simulation failure.

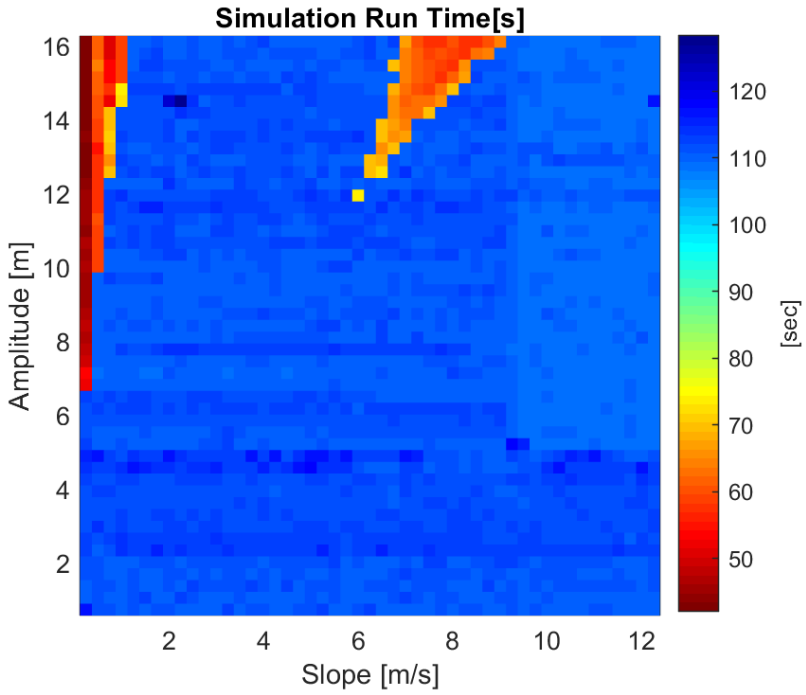

Figure 5-2. Slope-Amplitude simulation run time

Figure 5-3 shows the two types of simulation failure observed during the analysis. The capsize, left, is the result of an extremely low slope and large amplitudes. The plot on the bottom right corner shows a 14.5 m drop in wave elevation, causing the ship to rapidly lose stability by losing waterplane area and thus, capsizing. The failure to the right shows a vessel capsizing because of encountering multiple 14 m to 16 m waves at a frequency of 12 s.

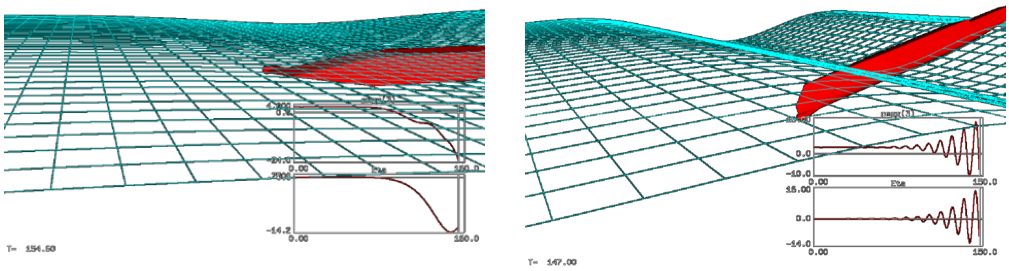

Figure 5-3. Types of simulation failure.

5.3.3 Response Map Adjustments

Though the intent was to reproduce realistic ocean waves, we found that certain combinations of amplitude and slope produced non-physical wave groups in LAMP, resulting in extreme response calculations that made it difficult to analyze the remaining portions of the response maps. Figure 5-4 shows the original response map for the heave force minima (left) and adjusted response map (right). The color gradient shows the change in the minimum measured heave force for each wave group, slope, and amplitude combination.

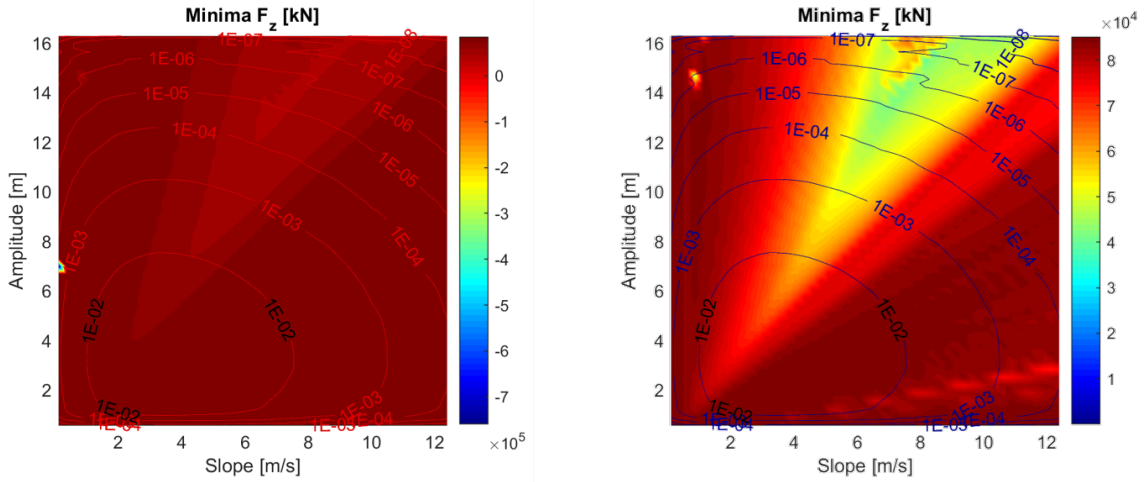

Figure 5-4. Improvement in by filtering out transient spikes.

The overlaid on the response map are contours the joint wave group probability, figure 4-10. Notice the outlier at the far left of the unadjusted heave force response map. Further inspection of this simulation showed an unexpectedly large start up transients, which were not related to the wave groups themselves, figure 5-5.

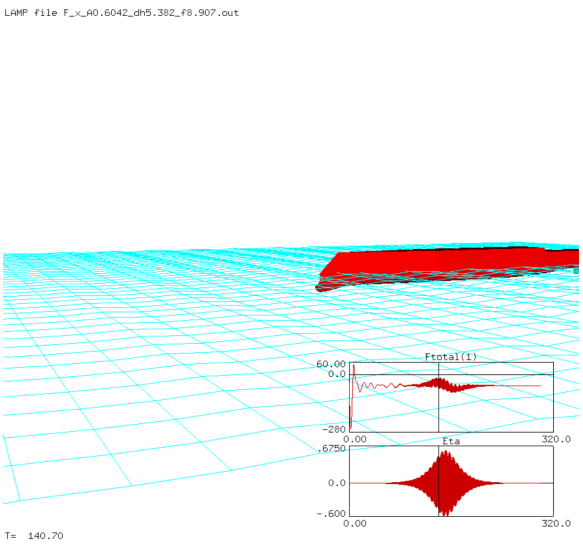

Figure 5-5. Unexpected heave response at low wave slope

Similar cases were present in other response parameters. To improve the resolution in the areas of interest, (center and top right of the response map), we smoothed out the effects of transients for slopes less than 0.7 m/s. This did not impact the distribution calculations, but allowed us to see the rest of the response map with greater detail. Further discussion on the physical meaning of these response maps is provided in Chapter 6.

Chapter 6

Analysis of Simulation Results

As briefly discussed in Chapter 5, results from the wave group sampling simulations were collected in response maps. Of the twelve output parameters considered, five produced interesting results for further analysis. In this chapter we discuss each of the response parameters individually.

The wave groups act as a threshold value, but to establish specification for operational limits or risk-based standards, it was necessary to consider the wave group probability map. Finally, we compared the PDFs of the slope-amplitude sampling simulations with the previously completed lengthscale-amplitude approach, as well as the Monte Carlo simulations. The forces, moments, and motion measured in the following simulations are with respect to the ship center of gravity.

6.1 Surge Force

Amplitude-Slope Wave Groups

The surge force, F_x, is the forward-aft force felt due to accelerations along the $x - axis$ of the ship. The ship was given a steady heading of 10 kn, so additional accelerations were introduced except those caused by the wave group. Figure 6-1 is the response maps from the slope simulations. The contour bands represent the joint probability of the wave group combination in a logarithmic scale.

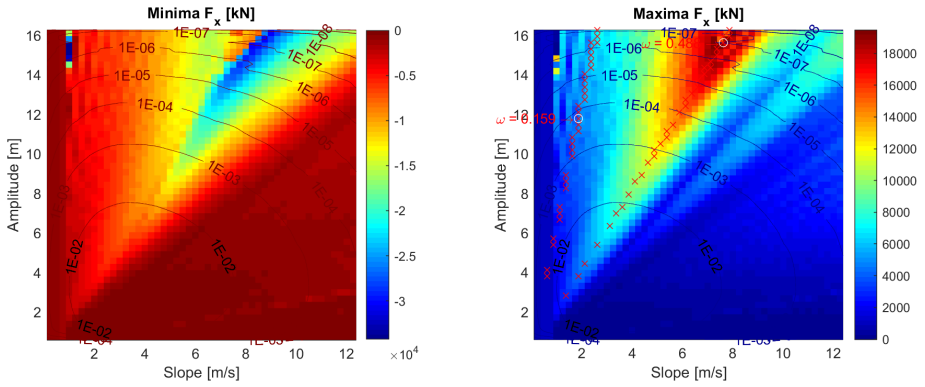

Figure 6-1. Surge Force Response Map of the Slope Simulation

Bands of constant heave force are clearly visible along the diagonals of the slope-amplitude response map. These bands align with lines of constant frequency, which were a product of calculations discussed in 3. The two regions where the simulation failed or capsized are also present in these maps. The filtering step, reduced the impact of the extreme values on the far left of the map, but the region at the top of the map with extreme values is still present. This extreme response area has very distinct edges resulting from resonance between the hull and the large wave group. Figure 6-2 shows a snapshot of the simulation highlighted by the white circle on the response map.

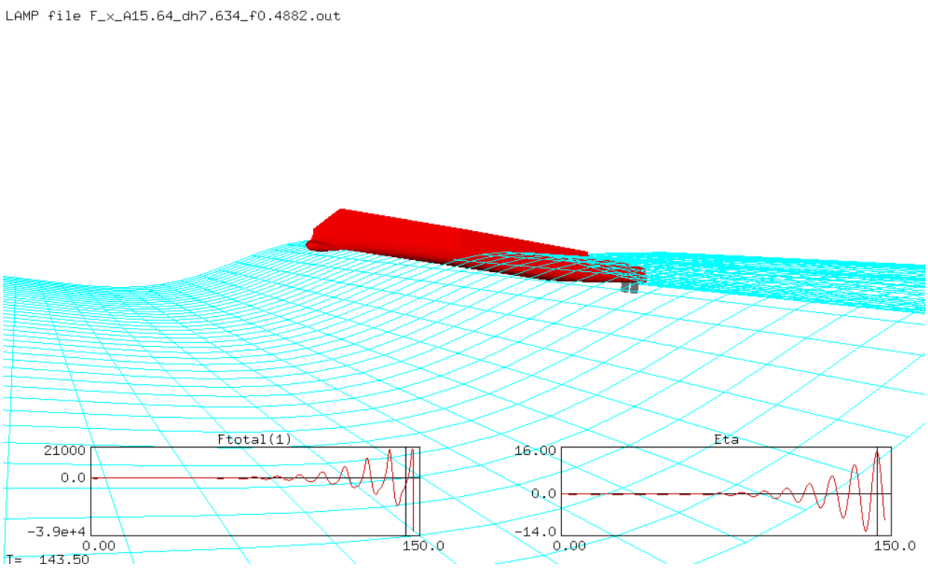

Figure 6-2. Wave Group Simulation A =15 m $\frac{d\eta}{dt}$ =7.63 m s^{-1}

This is an extreme sea way, and likely outside the operational limit of most sea going vessels. This wave is 15.6 m (50 ft) above the mean waterline and is categorized as Sea State 9 on the Douglas Scale, by the World Meteorological Organization (WMO). As noted by the probability contours, such waves systems are very rare and result from extreme hurricane conditions, with sustained winds over 67 kn. For reference, the bridge of an Arleigh Burke-class Destroyer sits 55 ft above the waterline.

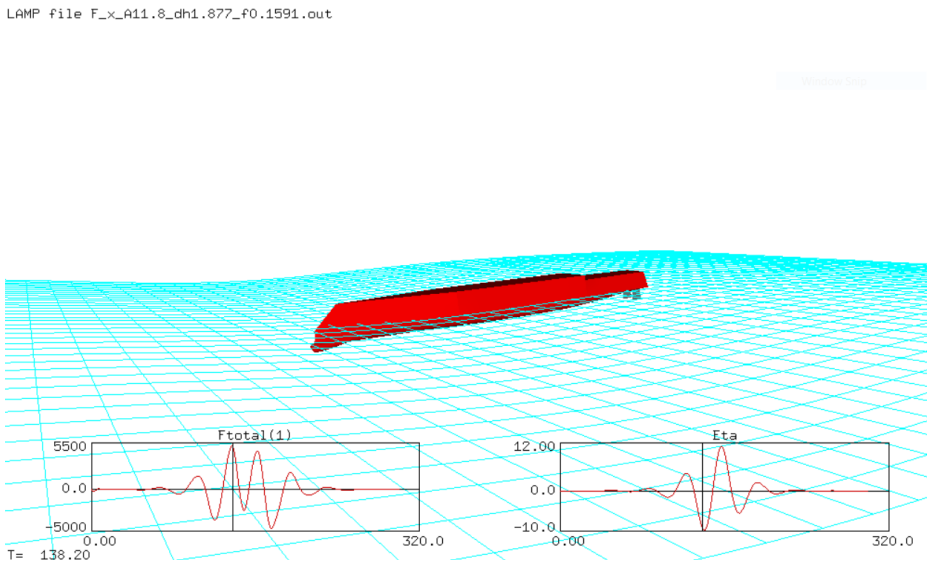

Figure 6-3. Wave Group Simulation A =12 m $\frac{d\eta}{dt}$ =1.88 m s^{-1}

For comparison, we considered a more modest wave group, shown in figure 6-3. This is still a relatively large wave system, with peak amplitude of 12 m (39 ft), but the peaks are much further apart than the overall length of the ship, so the extreme conditions goes almost unnoticed.

Response Distribution

We combined the response and probability maps from the sampling set to develop response distribution. The slope-versus-amplitude sampling set was compared to the Monte Carlo simulation, show in blue in figure 6-4, and lengthscale-versus-amplitude sampling set, shown in yellow. The middle row is in natural scale, while the bottom row is provided in a logarithmic scale in the y-axis. The Rayleigh distribution is also provided as a dashed line to show the Gaussian approximation. Since we are

considering only "extreme events," the PDFs are only provided for cases beyond two standard deviations from the mean value (further referred to as the "tail"). The gray vertical lines depict the mean (thick grey) and standard deviations (increasingly lighter gray lines).

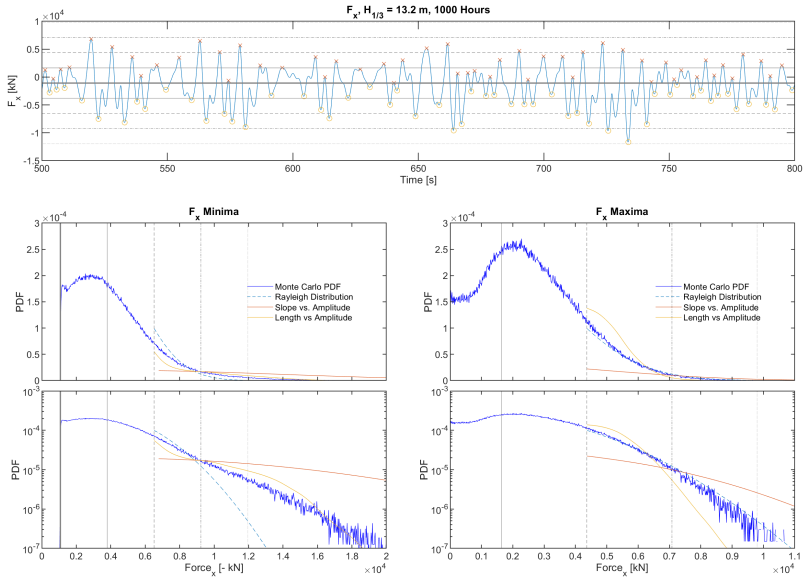

Figure 6-4. Surge Force Distribution

The slope-amplitude sampling set consistently over predicted the ships response in all loading conditions. The Rayleigh distribution under predicted the minimum surge force, suggesting a heavy tail structure. The lengthscale-amplitude sampling set remained the best fit for both responses. The slope simulations least accurate followed the shape of the Monte Carlo simulation.

6.2 Heave Force

The heave force, F_z, is the vertical force along the $z - axis$ of the ship. Figure 6-5 is the response maps from the slope-amplitude simulation set.

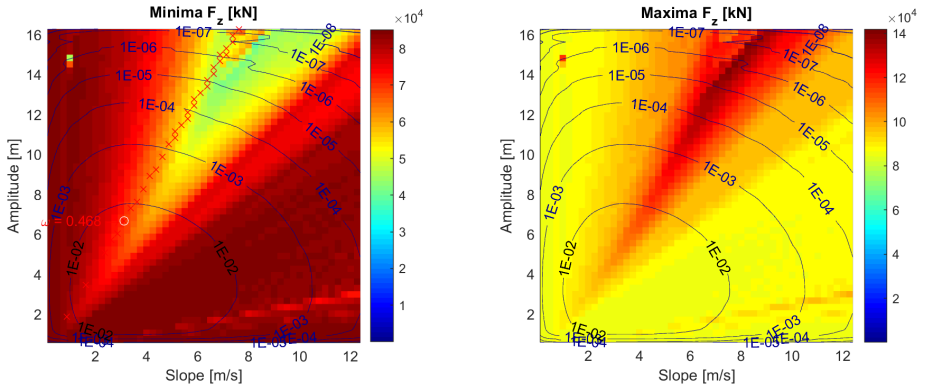

Figure 6-5. Heave Force Response Map of the Slope Simulation

For this response, we selected a simulation that fit a more realistic design limit within the first contour line. Highlighted by the white circle in the minimum surge force map, 6-6 shows 6.6 m (21 ft) wave system. This heave force is on the order of 100 kN (11 t), which would still be categorized as an extreme event for the ship structure, though, it did not result in a stability failure.

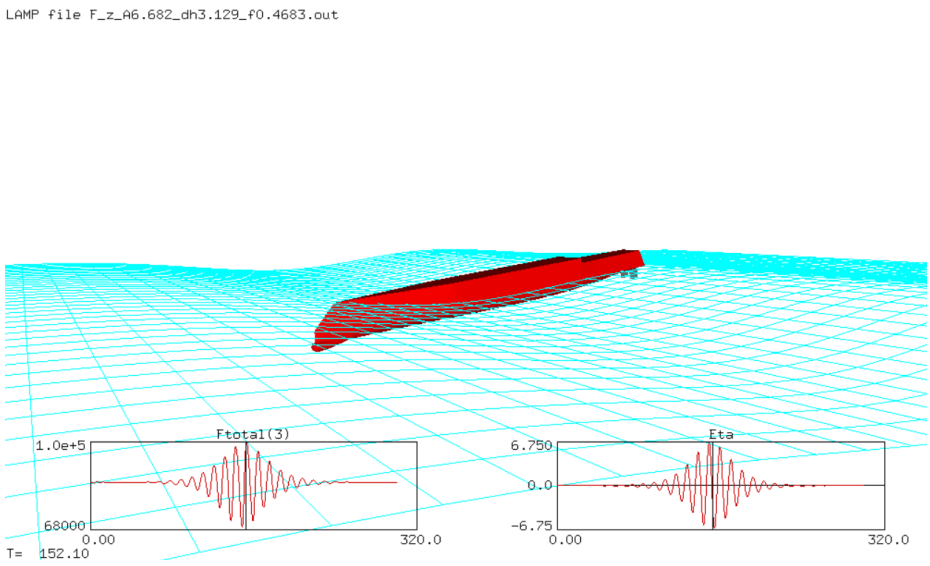

Figure 6-6. Wave Group Simulation A =6.6 m ω =0.47 rad s^{-1}

Moving forward, providing additional snapshots and response maps did not add significant value to this discussion, but are available for reference in Appendix B.

Response Distribution

Figure 6-7 shows PDFs for the heave force minimum and maximum. The length scale (LA) distribution performed best in the minimum force distribution. No specific distribution stood out as fitting the Monte Carlo distribution better in the maximum force distribution.

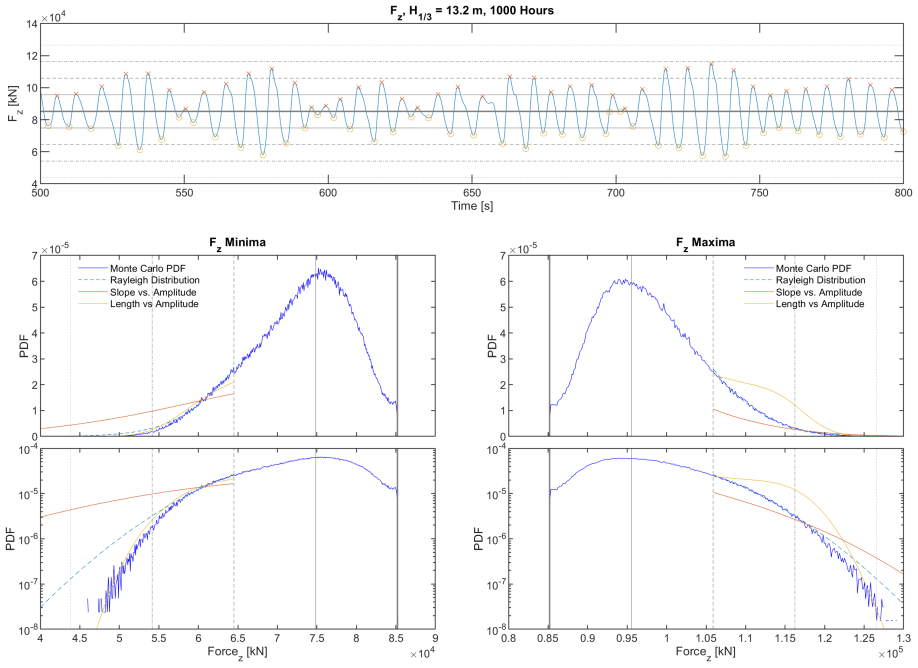

Figure 6-7. Heave Force Distribution

6.3 Heave Motion

Heave motion was measured as the vertical position of the ship center of gravity taken from its initial position at $t = 0$. Figure 6-8 shows the PDFs of the sampling sets. These results show no clear correlation between any wave group sampling set and the Monte Carlo distribution.

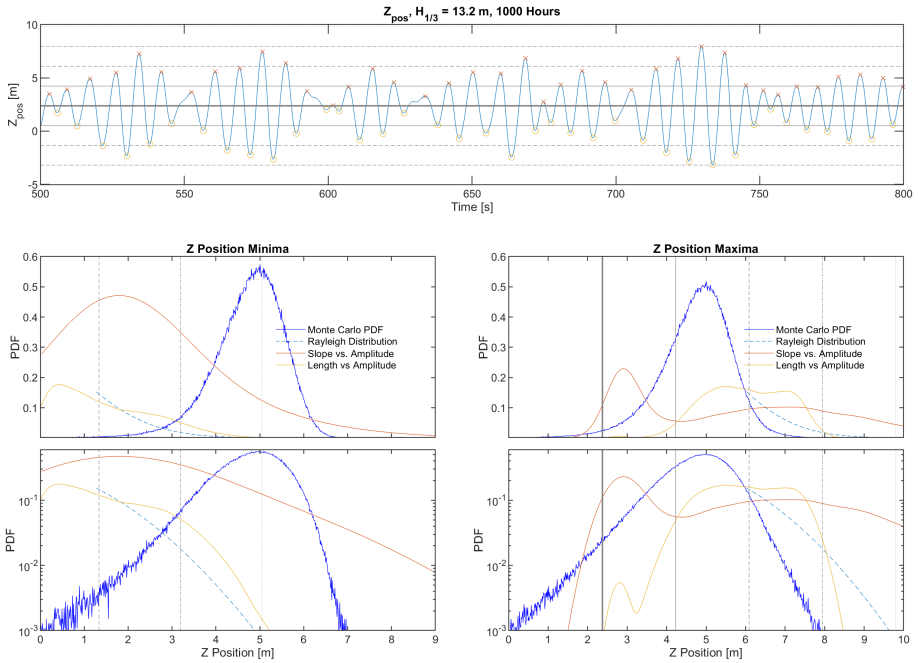

Figure 6-8. Heave Motion Distribution

6.4 Pitch Motion

Pitch is the rotation about the transverse or y-axis of the ship measured in degrees. The upward motion of the bow relative to the center of gravity is considered positive pitch or maxima. Figure 6-9 shows the PDFs of the sampling sets. The slope sampling more closely captured the shape of the Monte Carlo distribution than in previous response cased. In both the maximum and minimum, it was interesting to note that the slope sampling and the Rayleigh distribution, over predicted the weight of the tails.

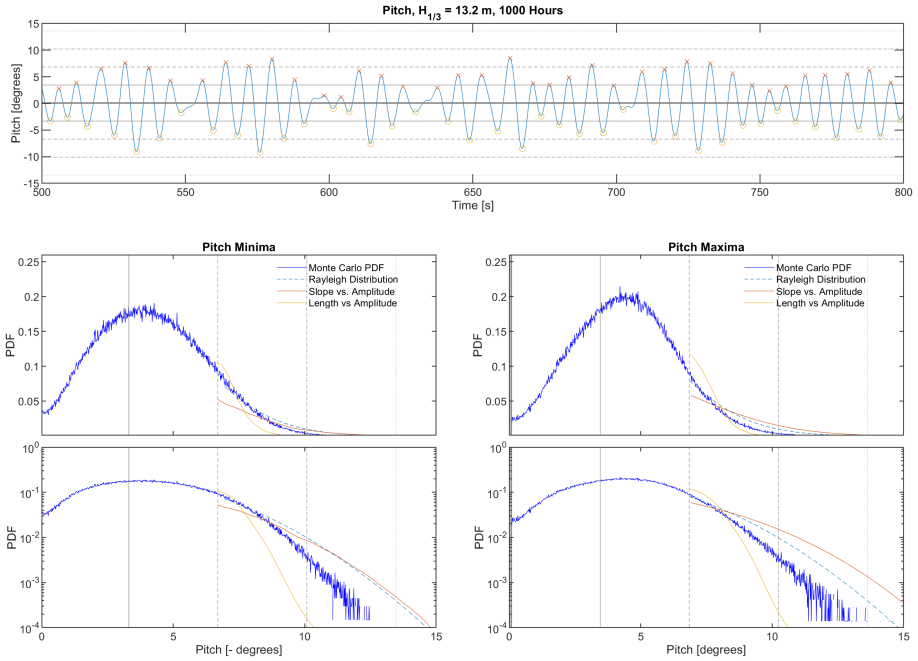

Figure 6-9. Pitch Motion Distribution

6.5 Pitching Moment

The final parameter we considered was the pitching moment, M_y. The minimum moment is in moment in the negative, bow-down direction. Figure 6-10 shows the PDFs for the wave group sampling sets. The slope-amplitude sampling approach was able to capture the shape of the Monte Carlo simulation only in the M_y minima case. Pitch and pitching moment were the main parameters we sought to capture with a new wave group sampling approach.

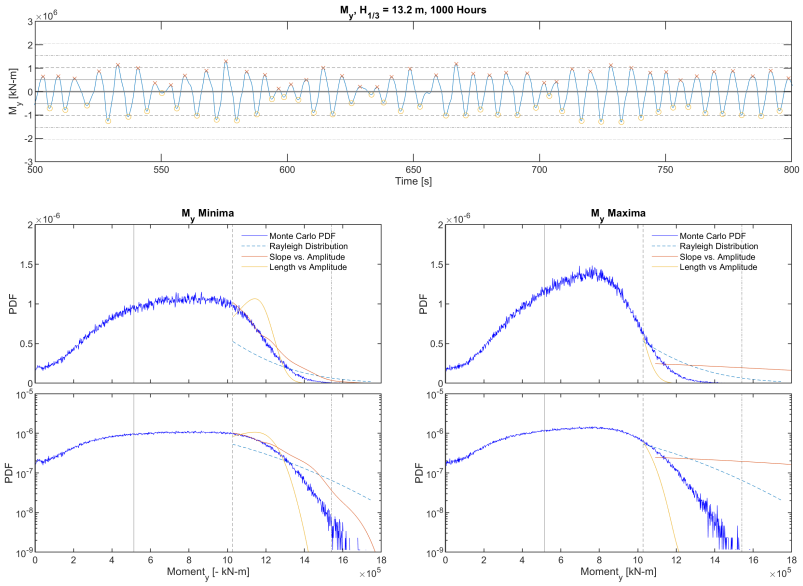

Figure 6-10. Pitching Moment Distribution

6.6 Summary

The slope-amplitude sampling distributions over predicted the response in all cases. Rather than capturing the maximum value of the response, we can bring the distribution closer to the Monte Carlo simulation by taking the average of the three or four highest values. This would be more representative of the entire wave system. Also, we can improve the sampling efficiency by taking into account wave steepness. Such high frequency wave systems do exist in nature but generally exotic waves. We had expected the joint distribution maps to make the effects of these combinations negligible, but ultimately, these systems impacted the final response parameters more than predicted.

Chapter 7

Industry Application

The aim of this analysis was characterizing the extreme events in terms of a series of short simulations that may be used for further analysis using high fidelity CFD or basin model testing. Though several discrepancies remained in our characterization of wave groups, a successful realization of this approach would provide a basis to know exactly the risk of each wave system and physically what the loads were going to be [8]. In this way, we would not only be able to reproduce the conditions that result in these rare events, but also understand the conditions associated with them.

Wave groups were incorporated for the first time, into the Second-Generation Intact Stability Criteria. This shifted the basis of stability criteria from accident statistics to physics-based. The new criteria are formulated in tiers, with the lower tier being focused on early stage designs and the follow-on stages requiring additional evaluation of "safety level" i.e. the probability of failure despite having satisfied the criterion [13].

7.1 Routing for Operational Efficiency

The successful application of the wave groups concept could provide ship operators and owners with a risk evaluation tool that incorporates operational loads into navigational routing decisions. Similar Decision Support Systems (DSS) already account for fuel efficiency and heavy weather avoidance. Figure 7-1 illustrates the decision

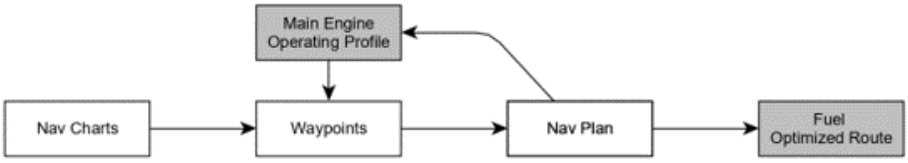

Figure 7-1. Route optimization for fuel efficiency

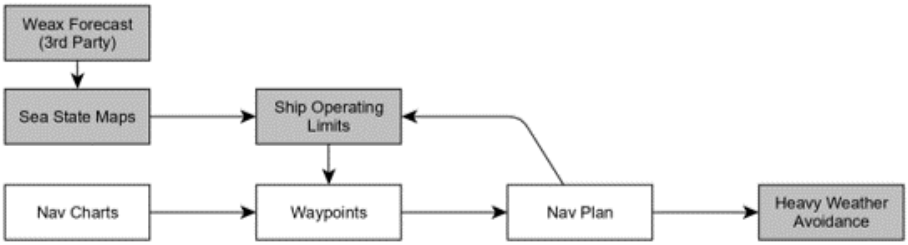

Figure 7-2. Route optimization for heavy weather avoidance

model for route planning on the basis of fuel efficiency. The iterative loop considers route waypoints and the operating profiles of the main engines to determine best course and speed. This is generally the first phase of route planning.

Concurrent to fuel routing, national weather services like the Nation Oceanic and Atmospheric Administration and the Navy Weather Center, provide weather update using national weather assets and observational data provided by other mariners. This information is generally passed along as sea state recommendation that can be correlated to the vessel‘s operational limits. These limits are predetermined during first-of-class rough water trials or through response amplitude operators (RAO) simulations. Figure 7-2 illustrates this decision model.

This is useful for pre-voyage route planning and providing updates along the way. However, this approach is limited to avoiding extreme excursions outside the operational profile. Papanikolaou et. al argued that for on board DSS to be truly practical for route optimization and risk mitigation, probabilistic assessment methods would need to replace traditional deterministic guidance models [19]. The Wave Group methodology offers just this. Weather data can be translated into wave group characteristics and overlaid on the navigational chart. Using a library of a pre-computed, standard set of wave groups and associated responses, the DSS is able

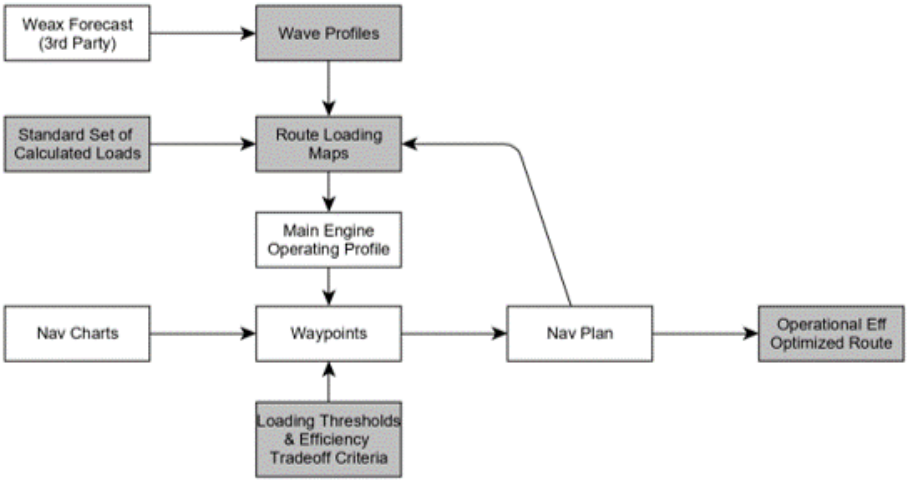

Figure 7-3. Route optimization for operational efficiency

to forecast operational loads directly on the navigational chart. Figure 7-3 illustrates this decision process. Ultimately, the operator sees a list of potential routes and filters. The filters are based on operational criteria that can reduce life-time fatigue and improve engine efficiency.

7.1.1 Stakeholder Analysis

We identified two primary stakeholders that would benefit from a such a DSS: The Navy and the commercial maritime industry. However, we found that their needs and how they would implement this system would be very different. Consider the operating profiles of a standard Naval combatant vessel and a loaded bulk cargo vessel, figure 7-4 [4, 5]. Navy ships operations are based on a larger mission set of training and deployments. During a deployment a vessel may need to rapidly reposition from one area to another and then loiter in that area until operational commanders provide further tasking.

In the case of commercial vessels, the operational tempo, though still demanding, is much more predictable. As shown in this speed profile, once the vessel has left port, the route and speed are well established. Commercial vessel operators also have the option to delay shipment in case of heavy weather or re-route to reduce extreme loads. For these reasons, both stakeholders are interested in very different ends of the

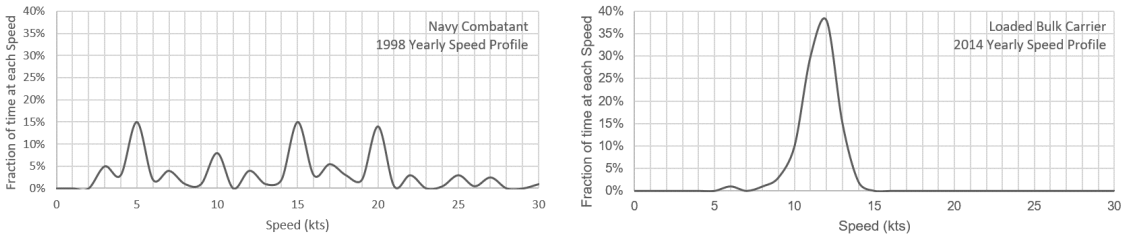

Figure 7-4. Annual speed profile for a US Navy combatant (left) and a loaded bulk cargo vessel (right) [4, 5]

trade space, figure 7-5, and realize the benefits of the Wave Group methodology and near-real-time risk evaluation in different ways.

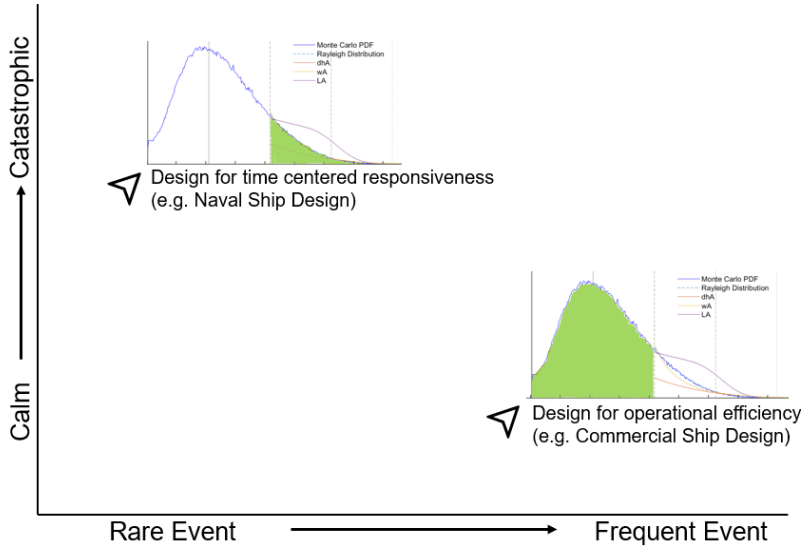

Figure 7-5. Operational efficiency routing tradespace and stakeholders

Navy designers seek to better understand the characteristics of extreme events so that they may account for the demanding operational loads from the conception of the design. Wave groups offers a physics-based model to replace existing mathematical models and reduce uncertainty for the extremely rare end of the distribution. In the end, if the current estimates over predict certain loading conditions, the specification can reduce plate thickness and weight. Alternatively, in the case current estimates under predict extreme events, actions can be taken to reduce further damage and potentially mitigate a total loss of a $1.8B surface combatant.

The commercial maritime industry, is a much large stakeholder in terms of shear numbers of vessels and annual miles traveled. The Wave Groups methodology opens and new type of routing for operational efficiency, which is applicable even in the absence of heavy weather. By correlating loading conditions to incident wave patterns, ship operators can develop routes that avoid the heaviest loads and reduce fatigue for their specific hull structures. Consider the transit between two of the busiest ports in the world, the Port of Shanghai, and the Port of Los Angeles, which are approximately 5,633 nautical miles apart [20]. Though modeling this fatigue analysis was beyond the scope of this work, the benefits could possibly add years to the service life of these vessels. In 2018, over 1800 vessel arrived at the port of Los Angeles, of which 73% were from China and neighboring countries [21]. The value of such an approach is only multiplied by these factors.

7.1.2 Technology Risk

With current technology, Navy and cargo vessels could be sufficiently instrumented to track loads and fatigue imposed on the hull during normal operation. This data would then be used to improve the current wave groups theory and vice versa, a successful wave groups model could identify deviation in normal operational loads as means of predicting failure. The estimation of sea state parameters on the moving ship remains a fundamental problem to be solved [19]. Wave groups also offer an alternative to full scale wave prediction by reducing the scope to the prediction of smaller sets; however, this work is still theoretical.

Nearly a decade ago, attempts to capture wave elevation in real time used X-band radars to map the wave elevation and while simultaneously recording the non-linear motion of the ship with accelerometers. Unfortunately, the ship does not perform like a buoy and many efforts like this over the past decade have tried and failed to reconcile this problem. The most recent developments of sea state sensing were completed from a shore facility in Istituto per l'mbiente Marino Costiero (IAMC) of the Italian National Research Council in 2017 [22]. Other recent efforts have applied machine learning and neural networks to help quantify extreme events in ship response, but

training these systems has proved challenging because the ocean environment changes too drastically from the training area to the operational area. In the interim, the National Oceanic and Atmospheric Administration (NOAA) continues the densely monitor the world‘s oceans. Wave elevation by buoy and wind data are still the best predictors of heavy weather.

7.2 Risk Mitigation with Digital Twin

An innovative application is in the development of a shore based digital twin. If the wave group approach can quantify risk in near-real-time, operators and ship owners have the opportunity, via a digital twin, to determine the real risk of a vessel at sea. This would provide a more definitive way of understanding risk beyond sea states and polar plots, which are used today. Wave groups would provide a catalog of precomputed responses to the wave systems and in real time understand the conditions the ship is in and what is the probability of response events.

7.3 Ship Design and Model Testing

Once an approach is accepted, reproducing the wave groups in the Maneuvering and Seakeeping (MASK) Basin is straight forward. Instead of running weeks of model tests in the basin to evaluate a new design, the design team can run the set of waves known to lead to instabilities [11]. With the probability of these waves groups occurring in a certain sea state in a given area, these sets can be easily accommodated into heave weather guidance systems.

Chapter 8

Conclusions & Recommendations for Future Work

An approach to the construction of wave groups by characterizing slope and amplitude are presented in this study. In all cases, the response distributions over predicted the Monte Carlo simulation, which could be caused by several aspects data processing approach. It is possible that rather than selecting the largest response, using the average of a few of the most pronounced peaks could bring down the tails. From the sampling perspective, a more rigorous method for filtering out non-physical waves using parameters such as steepness could be implemented prior to the mLAMP simulations. This would reduce the number of simulations required, saving memory and time. Several MATLAB tools were provided to aid in the continued analysis of wave groups and mLAMP simulations. The final results of this wave group study were compared to direct Monte Carlo quantification and an amplitude-length-scale characterization of wave groups. Neither slope nor lengthscale approaches stood out as exclusive solutions to characterize the non-linear responses. The vertical position results in both cases were completely inconsistent, it would be worth exploring how this data was collected. Overall, the Wave Group methodology not only shows promise for both the quantification of extreme events, it also has potential the potential to improve tools for operational efficiency routing.

8.1 Future Work

Several opportunities for future work exist. The slope-amplitude probability map, consistently over predicted the Monte Carlo distribution. Rather than tracking the peak response amplitude, it would be worth taking the average of the top three or so peaks for each wave group time series rather than just the maximum value. There is an implementation of a mean crossing function that was used during the full Monte Carlo data analysis that would need to be implemented in the *LAMPout.m* script for each response parameter.

This and the previous application of wave groups to quantify ship response statistics simplified the probability space into two dimensions. Stevens characterized the wave groups by lengthscale and amplitude. Here, we characterized the wave groups by slope and amplitude. A final attempt would re-capture the lengthscale distribution to produce a three-dimensional probability space. This a heavier problem computationally, but this effort could reduce that burden with a more deliberate sampling approach. Instead of evenly spacing samples across the PDF. It is possible to spread out samples at low probability regions of the PDF, while also filtering out non-physical or exotic wave groups.

One of the applications, in discussion with the project sponsors, was the improvement in model testing time. Future work might consider combining the LAMP wave group simulation with model testing at the MIT tow tank.

Appendix A

LAMP Modification

Pefromed by Stevens in 2017 and provided as a reference [15].

One of the LAMP seaway inputs is for a superposition of sinusoidal waves with surface elevations of the form [17]:

$$\eta(x, y, t) = \sum_{n=1}^{N} A_n \cos(k_n(x \cos \beta_n + y \sin \beta_n) - \omega_n t + \theta_n).$$

These waves are similar to the desired form, and were identified as a good starting point. The primary modification was the inclusion of the windowing function S displayed in Figure

$$\eta^*(x, y, t) = S(x) * \zeta(x, y, t).$$

$$S(x) = sech(\frac{x}{L}) = \frac{1}{\cosh(\frac{x}{L})} = \frac{2}{\exp(\frac{-x}{L}) + \exp(\frac{x}{L})}.$$

The author obtained the LAMP source code and identified the files governing the wave input functions. The windowing function was added into the incident wave elevation function. While the experiment calls for a single wave input, the function was left in the summation form to avoid unnecessarily modifying the code. The incident wave elevation was therefore modified to:

$$\eta(x,y,t) = \sum_{n=1}^{N} A_n sech(\frac{x}{L}) \cos(k_n(x\cos\beta_n + y\sin\beta_n) - \omega_n t + \theta_n).$$

As long as only a single incident wave input is recieved, N will be equal 1, and this equation would revert to the desired input function:

$$\eta(x,y,t) = Asech(\frac{x}{L}) \cos(k(x\cos\beta + y\sin\beta) - \omega t + \theta).$$

The length scale input into the modified version of LAMP was separate from the wave input file, therefore only a single length scale can be used even if the analysis of several linear waves is deemed important.

As stated previously, LAMP does most of its calculations using the potential function. Within the superposition of sinusoidal waves seaway input, the potential function is calculated as:

$$\Phi(x,y,z,t) = \sum_{n=1}^{N} \frac{A_n g}{\omega_n} \exp^{k_n z} \sin(k_n(x\cos\beta_n + y\sin\beta_n) - \omega_n t + \theta_n).$$

This function also needed modification to include the windowing function:

$$\Phi^*(x,y,z,t) = S\Phi(x,y,z,t).$$

Which for a single sinusoidal wave input can be simplified to:

$$\Phi^*(x,y,z,t) = \frac{Ag}{\omega} sech(\frac{x}{L}) \exp^{kz} \sin(k(x\cos\beta + y\sin\beta) - \omega t + \theta).$$

Additional modifications were made to the time and spatial derivatives of the potential function ϕ and incident wave elevation function η. The result of these modifications was

Appendix B

Complete List of Simulation Figures

Surge Force F_x

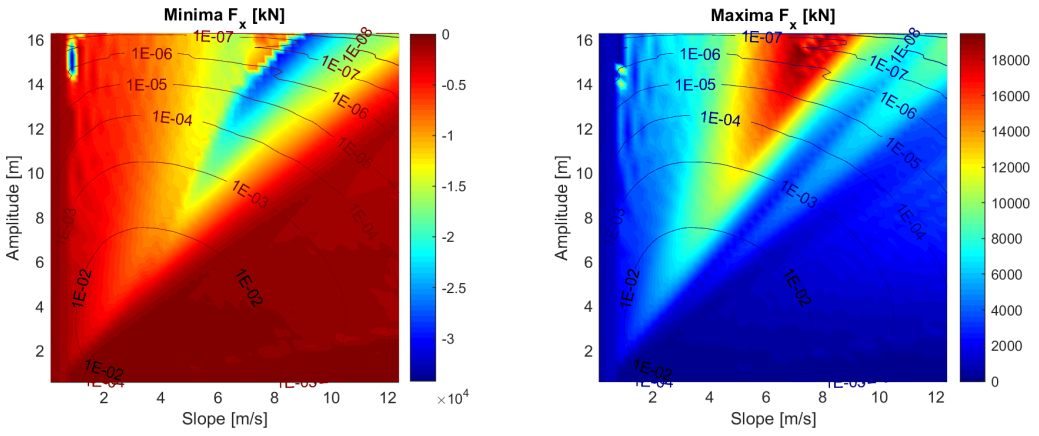

Figure B-1. Surge Force Response Map - Slope

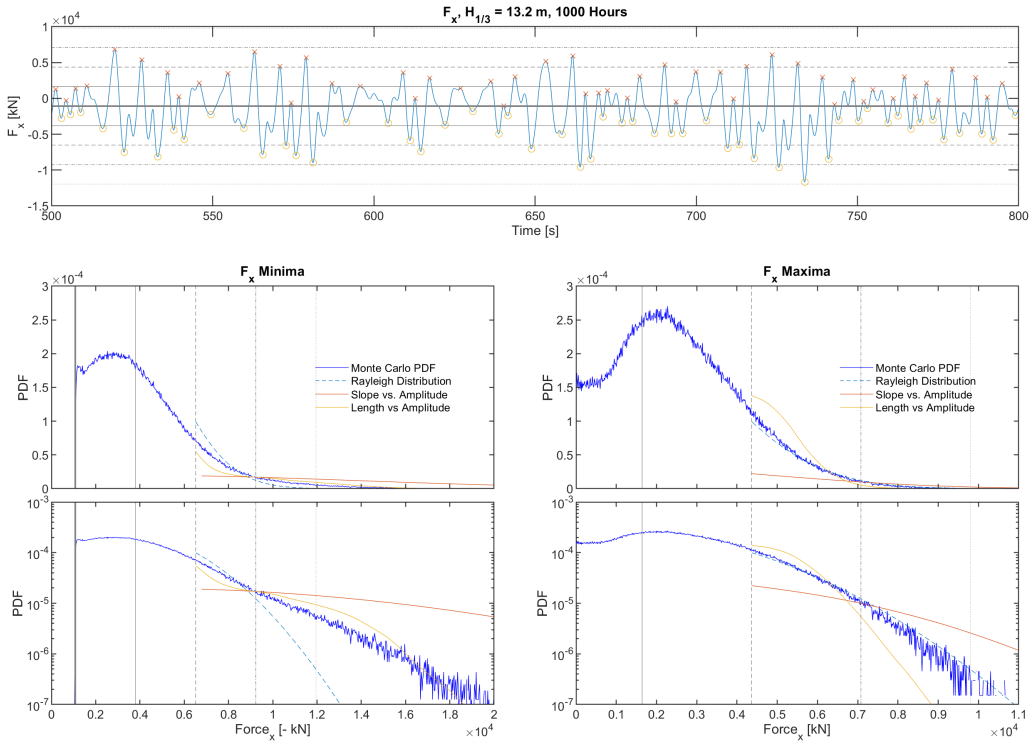

Figure B-2. Surge Force Distribution

Heave Force F_z

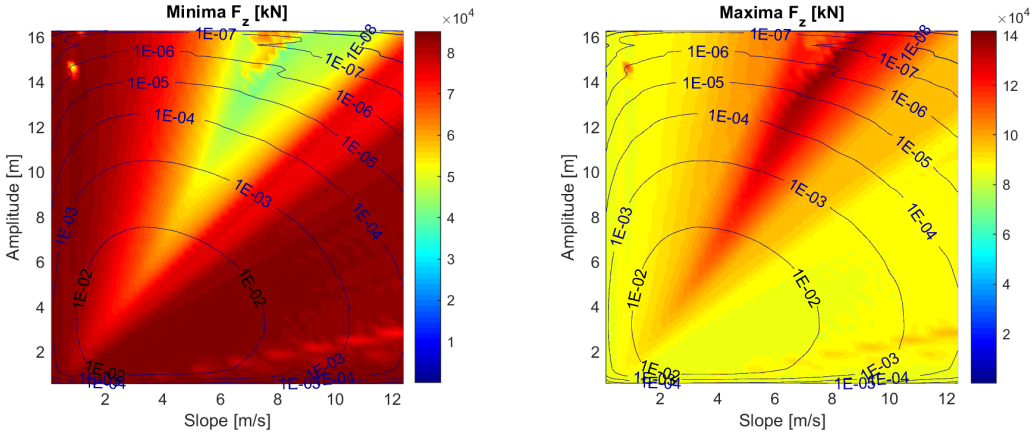

Figure B-3. Heave Force Response Map - Slope

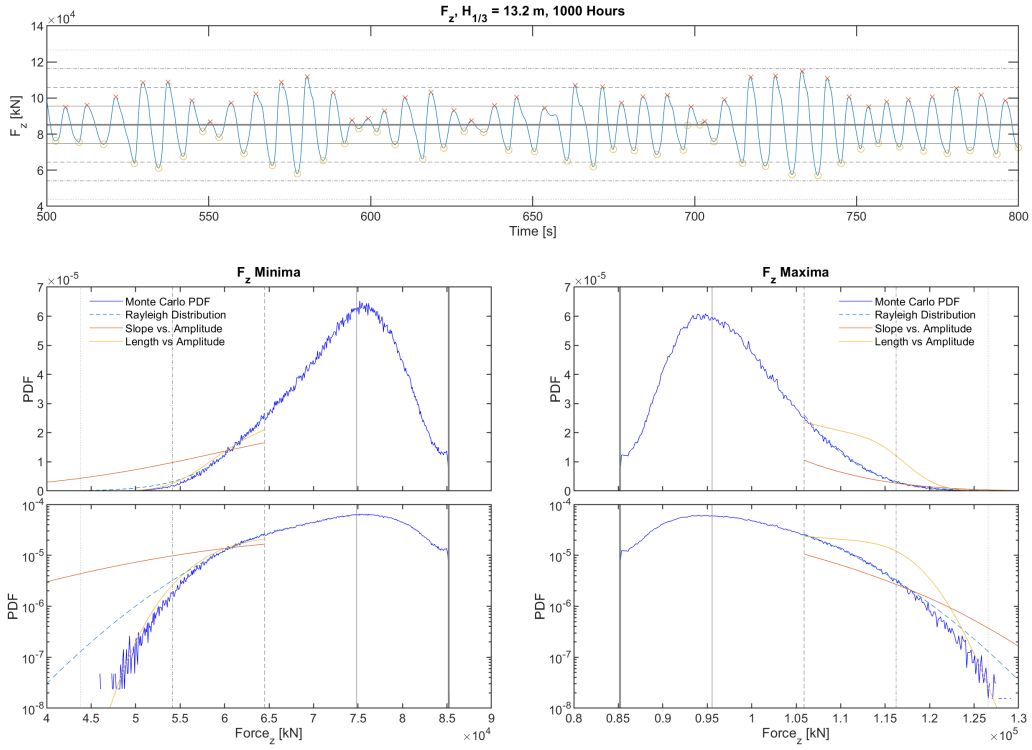

Figure B-4. Heave Force Distribution

Pitching Moment M_y

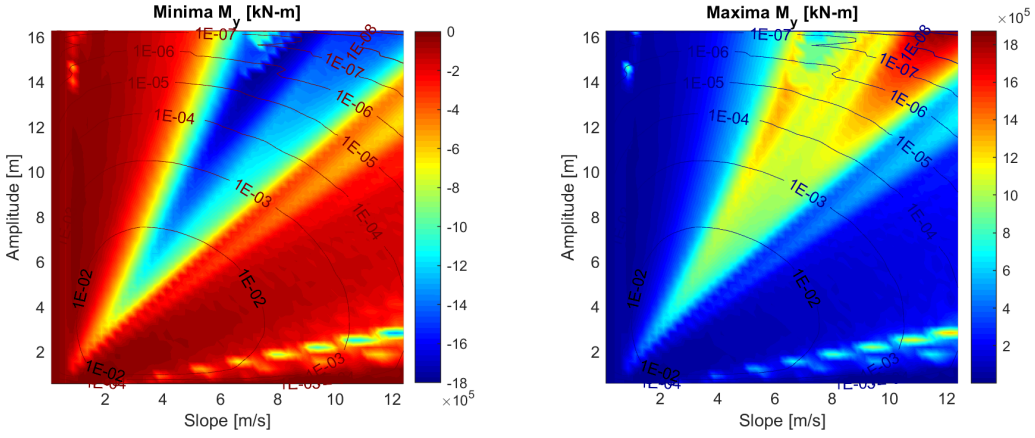

Figure B-5. Pitching Moment Response Map - Slope

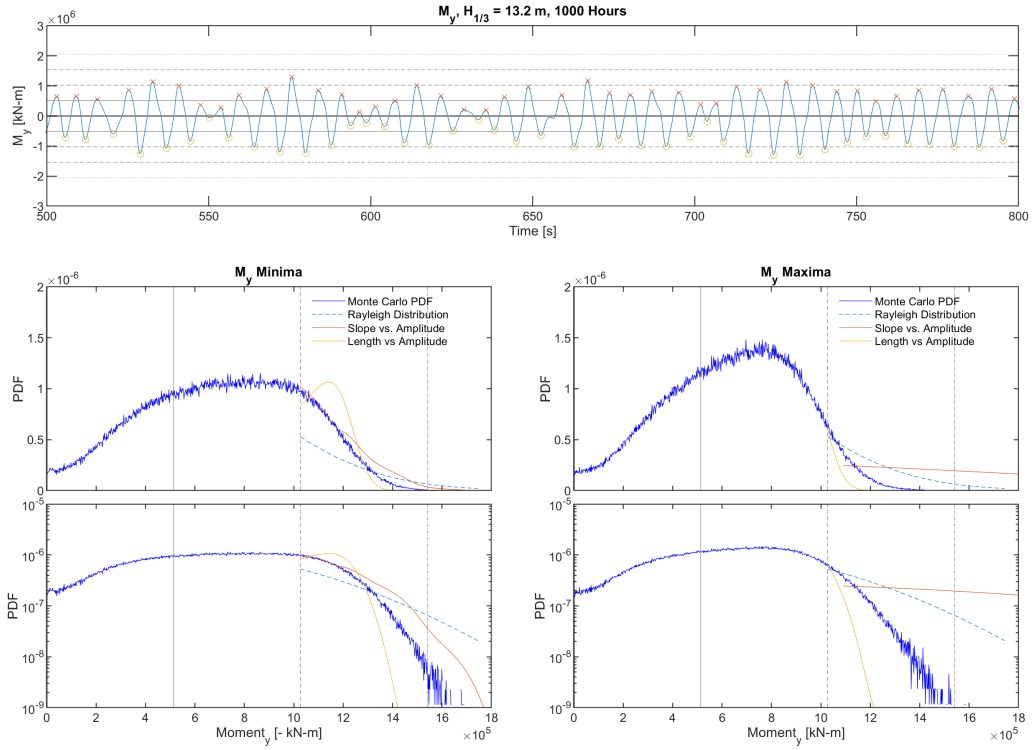

Figure B-6. Pitching Moment Distribution

Pitch Y_{rot}

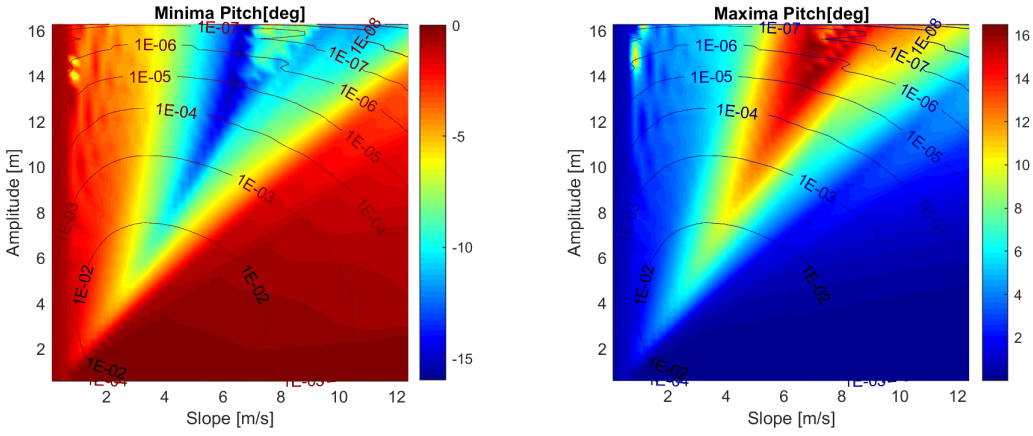

Figure B-7. Pitch Response Map - Slope

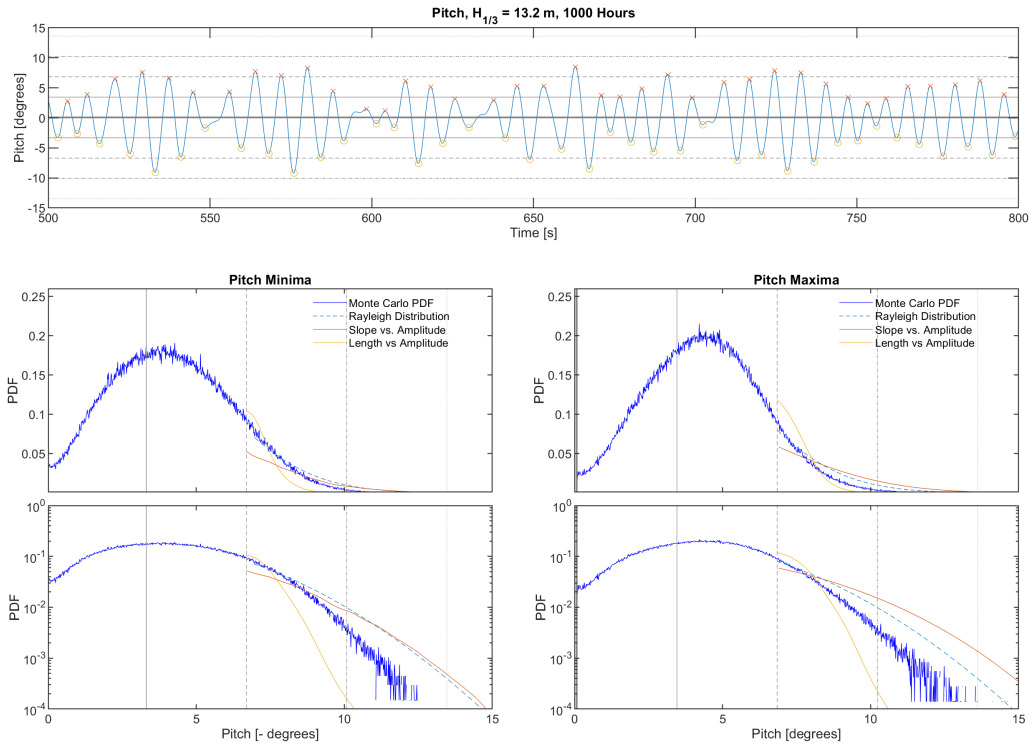

Figure B-8. Pitch Distribution

Heave Motion Z_{pos}

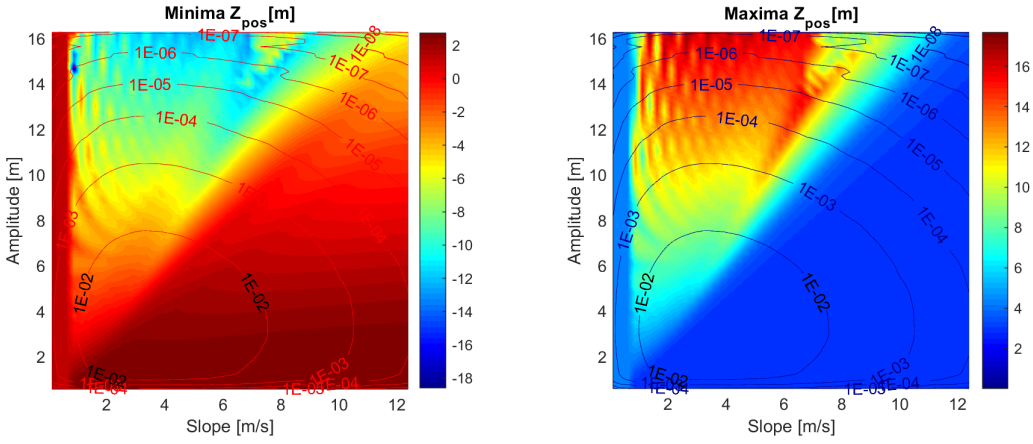

Figure B-9. Heave Motion Response Map - Slope

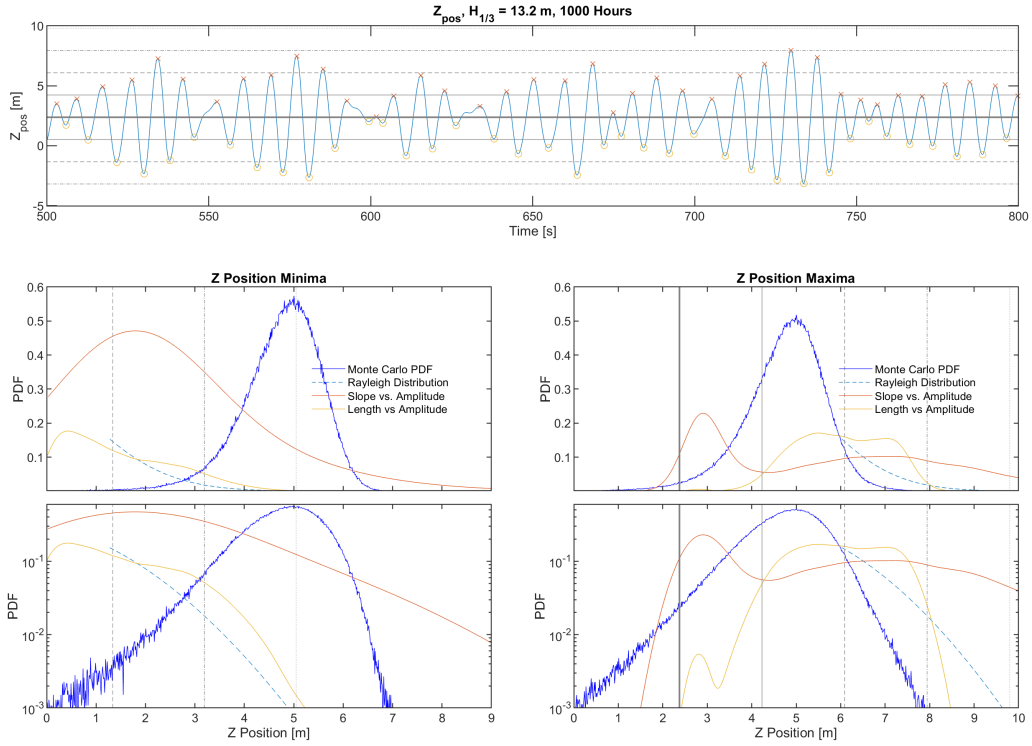

Figure B-10. Heave Motion Distribution

Bibliography

[1] C. Guedes Soares, A. Jasionowski, J. Jensen, D. Mcgeorge, A. D. Papanikolaou, E. Poylio, P. C. Sames, and R. Skjong, *Risk-Based Ship Design: Methods, Tools and Applications*, 1st ed., A. D. Papanikolaou, Ed. Berlin, Heidelberg: Springer Berlin Heidelberg, 2009. [Online]. Available: http://link.springer.com/10.1007/978-3-540-89042-3

[2] Department of Defense, "Operation of the Defense Acquisition System," pp. 1–23, 2003.

[3] H. E. Saunders, S. Carpenter, D. D. Hayden, and J. G. H. Iii, "Harold E. Saunders Maneuvering and Seakeeping (MASK) Facility New Directional Wavemaker," Bethesda, MD, 2015.

[4] C. S. Surko and M. Osborne, "DDG 51 Operating Speed Profiles and the Ship Design Cycle," *Naval Engineers Journal*, pp. 79–85, 2005.

[5] C. Banks, O. Turan, A. Incecik, G. Theotokatos, S. Izkan, and C. Shewell, "Understanding ship operating profiles with an aim to improve energy efficient ship operations," University of Starthclyde, Tech. Rep., 2014. [Online]. Available: https://www.onthemosway.eu/wp-content/uploads/2015/06/D5.1.Understanding-ship-operations.pdf

[6] International Maritime Organization (IMO), "Final Recommendation from research project HARDER," International Maritime Organization, Tech. Rep., 2003. [Online]. Available: http://projects.dnv.com/harder{_}ext

[7] International Towing Tank Conference, "Description and Rules of the ITTC," 2017. [Online]. Available: https://ittc.info/about-ittc/rules/

[8] K. M. Weems, "Phone Interview," 2019.

[9] M. S. Triantafyllou and F. S. Hover, "Maneuvering and Control of Marine Vehicles (13.49)," *Massachusetts Institute of Technology*, 2004. [Online]. Available: http://ocw.mit.edu/courses/mechanical-engineering/2-154-maneuvering-and-control-of-surface-and-underwater-vehicles-13-49-fall-2004/lecture-notes/1349{_}notes.pdf

[10] W. Cousins and T. P. Sapsis, "Unsteady evolution of localized unidirectional deep-water wave groups," *Physical Review E - Statistical, Nonlinear, and Soft Matter Physics*, vol. 91, no. 6, pp. 1–5, 2015.

[11] V. Belenky, "Phone Interview," 2019.

[12] C. Breinholt, K.-C. Ehrke, A. Papanikolaou, P. C. Sames, R. Skjong, T. Strang, D. Vassalos, and T. Witolla, "SAFEDOR-The Implementation of Risk-based Ship Design and Approval," *Procedia - Social and Behavioral Sciences*, vol. 48, pp. 753–764, jul 2012. [Online]. Available: https://linkinghub.elsevier.com/retrieve/pii/S1877042812027899www.sciencedirect.com

[13] P. A. Anastopoulos, K. J. Spyrou, C. C. Bassler, and V. Belenky, "Towards an improved critical wave groups method for the probabilistic assessment of large ship motions in irregular seas," *Probabilistic Engineering Mechanics*, vol. 44, pp. 18–27, apr 2016. [Online]. Available: https://www.sciencedirect.com/science/article/pii/S0266892015300709

[14] *International Code on Intact Stability, 2008*, 2009th ed. London, UK: International Maritime Organization, 2009.

[15] K. Stevens, "Adaptive Sequential Sampling for Extreme Event Statistics in Ship Design," Ph.D. dissertation, Massachusetts Institute of Technology, Cambridge, MA, 2018.

[16] P. Bocccotti, *Wave Mechanics of Ocean Engineers*, 1st ed., D. Halpern, Ed. Reggio-Calabria: Elsevier B.V., 2000.

[17] Leidos, *Large Amplitude Motions Program (LAMP) User's Guide*, 4th ed. Leidos, 2018.

[18] M. A. Mohamad, "Direct and adaptive quantication schemes for extreme event statistics in complex dynamical systems," Ph.D. dissertation, Massachusetts Institute of Technology, 2017.

[19] A. Papanikolaou and E. Alfred Mohammed, "Stochastic uncertainty modelling for ship design loads and operational guidance," *Ocean Engineering*, vol. 86, pp. 47–57, aug 2014. [Online]. Available: https://www.sciencedirect.com/science/article/pii/S0029801814000237

[20] J. A. Byers, "Great Circle Distance Calculator," 1997. [Online]. Available: http://www.marinewaypoints.com/learn/greatcircle.shtml

[21] Port of Los Angeles, "Facts and Figures," 2019. [Online]. Available: https://www.portoflosangeles.org/business/statistics/facts-and-figures

[22] G. Ludeno, F. Raffa, F. Soldovieri, and F. Serafino, "X-Band Radar for the Monitoring of Sea Waves," *Geosci. Instrum. Method. Data Syst*, 2017. [Online]. Available: https://www.geosci-instrum-method-data-syst-discuss.net/gi-2016-42/gi-2016-42.pdf